

ÉCOLE DE TECHNOLOGIE SUPÉRIEURE
UNIVERSITÉ DU QUÉBEC

THESIS PRESENTED TO
ÉCOLE DE TECHNOLOGIE SUPÉRIEURE

IN PARTIAL FULFILLEMENT OF THE REQUIREMENTS FOR
A MASTER'S DEGREE WITH THESIS IN ELECTRICAL ENGINEERING
M. A. SC.

BY
Alireza KHANIZADEH

A NOVEL APPROACH TO STATIC VOLTAGE STABILITY ANALYSIS

MONTREAL, MARCH 27, 2015

© Copyright Alireza Khanizadeh, 2015 All rights reserved

© Copyright

Reproduction, saving or sharing of the content of this document, in whole or in part, is prohibited. A reader who wishes to print this document or save it on any medium must first obtain the author's permission.

BOARD OF EXAMINERS
THIS THESIS HAS BEEN EVALUATED
BY THE FOLLOWING BOARD OF EXAMINERS

Mr. Pierre-Jean Lagacé, Thesis Supervisor
Department of Electrical Engineering at École de technologie supérieure

Mr. Maarouf Saad, Thesis Co-supervisor
Department of Electrical Engineering at École de technologie supérieure

Mr. Ambrish Chandra, Chair, Board of Examiners
Department of Electrical Engineering at École de technologie supérieure

Mr. Louis A. Dessaint, Member of the jury
Department of Electrical Engineering at École de technologie supérieure

THIS THESIS WAS PRESENTED AND DEFENDED
IN THE PRESENCE OF A BOARD OF EXAMINERS AND THE PUBLIC
MARCH 27, 2015
AT ÉCOLE DE TECHNOLOGIE SUPÉRIEURE

ACKNOWLEDGMENTS

There are no proper words to convey my deep gratitude and respect for my thesis and research advisor, Professor Pierre-Jean Lagacé. He taught me the skills to successfully formulate and approach a research problem. I would also like to thank him for being an open person to ideas, and for encouraging and helping me to shape my interest and ideas.

I would like to express my deep gratitude and respect to Professor Maarouf Saad, my co-supervisor whose advices and insight was invaluable to me. He generously provided me constructive criticism, which helped me develop a broader perspective to my thesis.

I would like to thank my family, especially my parents and wife for always believing in me, for their continuous love and their supports in my decisions. Without them, I could not have made it here.

Thanks to my supportive friends in GRÉPCI laboratory, Hashem, Arvin, Mahdi, Hamed, Hassan, Hani, Jeffrey and others who made the lab a friendly environment for working.

UNE APPROCHE NOUVELLE D'ANALYSE DE LA STABILITÉ STATIQUE DE LA TENSION

Alireza KHANIZADEH

RÉSUMÉ

Un nouvel indice pour évaluer la stabilité de tension est présenté dans cette mémoire. L'indice proposé contient des informations utiles pour l'analyse de la stabilité de la tension comme des marges de stabilité de tension ainsi que les statuts de contrôlabilité de tension de tous les bus de charge. Un algorithme de perturbation et d'observation (P & O) est utilisé pour suivre les marges de capacité de charge maximale de tous les bus de charge. Les statuts de tension contrôlabilité de chaque bus est examinée en utilisant la sensibilité de l'amplitude de tension à l'injection de puissance réactive sur le même bus. La sensibilité puissance-tension réactif peut être extraite de l'inverse de la matrice jacobienne utilisée dans la résolution d'équations de flux de puissance par la méthode de Newton-Raphson. La thèse explique d'abord les concepts de base de la stabilité de la tension et de la capacité de charge maximale avec les définitions et les classifications de stabilité de la tension et les conditions qui conduisent à l'instabilité de tension. Une brève description de la L-indice qui est l'une des approches conventionnelles les plus largement utilisés à la tension évaluation de la stabilité est ensuite présentée avec les résultats de simulation de cette technique. La relation entre la capacité de charge maximale et Thevenin impédance est discuté suivante. Les étapes pour développer la stabilité de tension proposé et Capacité de charge (VSL) indice sont ensuite expliqués. Elle est suivie par une discussion sur les résultats de la simulation et la comparaison entre les résultats obtenus à partir de l'indice de VSL et ceux de obtenue à partir de l'approche du L-index. Depuis les cas de test comprennent des grands réseaux électriques, tous les résultats ne ont pas été présentées dans le chapitre sur les résultats de simulation. Les résultats détaillés des deux études de cas sont présentées dans les Annexes. Les résultats montrent la précision et la robustesse de l'indice de VSL sur la L-index. Les résultats confirment également que l'indice de VSL fournit une mesure précise de la tension à proximité de l'instabilité. Le dernier chapitre contient une conclusion de l'étude et des recommandations pour les travaux futurs.

Mots clés: Courbe P-V, Courbe P-Q, Impédance de Thévenin, La stabilité de la tension, Marge Capacité de charge, Matrice Jacobienne.

A NOVEL APPROACH TO STATIC VOLTAGE STABILITY ANALYSIS

Alireza KHANIZADEH

ABSTRACT

A novel index to assess voltage stability is presented in this thesis. The proposed index contains useful information for voltage stability analysis such as voltage stability margins as well as the voltage controllability statuses of every load buses. A perturbation and Observation (P&O) algorithm is utilized to track the maximum loadability margins of all load buses. The voltage controllability status of each bus is examined using the sensitivity of the voltage magnitude to the injection of reactive power to the same bus. The reactive power-voltage sensitivity can be extracted from the inverse of the Jacobian matrix used in solving power flow equations by Newton-Raphson method. The thesis first explains the basic concepts of voltage stability and maximum loadability along with definitions and classifications of voltage stability and the conditions which lead to voltage instability. A brief description of L-index which is one of the most widely used conventional approaches to voltage stability assessment is then presented along with simulation results of this technique. The relationship between maximum loadability and Thevenin impedance is discussed next. The steps to develop the proposed Voltage Stability and Loadability (VSL) index are then explained. This is followed by a discussion of the simulation results and comparison between the results obtained from the VSL index and those of obtained from the L-index approach. Since the test cases consist of large power systems, all the results have not been presented in the chapter on simulation results. The detailed results of two case studies are presented in the Appendices. The results show the accuracy and robustness of the VSL index over the L-index. The results also confirm that the VSL index provides a precise measure of proximity to voltage instability. The final chapter contains a conclusion of the study and recommendations for future works.

Keywords: Jacobian matrix, Loadability margin, PV curve, QV curve, Thevenin impedance, Voltage stability.

TABLE OF CONTENTS

	Page
INTRODUCTION	1
CHAPTER 1 VOLTAGE STABILITY	7
1.1 Voltage stability definition	7
1.2 Mechanisms of voltage instability	8
1.2.1 Insolvability of the power flow equations	8
1.2.2 Loss of Voltage Controllability	10
1.3 Loadability limit vs Loadability margin	12
1.4 Classification of voltage stability.....	12
1.5 Relationship between power transfer and voltage (Mahseredjian 2012).....	13
CHAPTER 2 L-INDEX	19
2.1 Simulation Results	20
2.1.1 Case 1: IEEE 118-Bus	20
2.1.2 Case 2: Hydro-Quebec network.....	21
2.1.3 Case 3: 2736-Bus system	22
CHAPTER 3 RELATIONSHIP BETWEEN THE MAXIMUM LOADABILITY AND THEVENIN IMPEDANCE	23
3.1 Relationship between PV curve and load's apparent impedance	23
3.2 Generalization to n-bus system.....	27
CHAPTER 4 PROPOSED VOLTAGE STABILITY ASSESSMENT TECHNIQUE ..	31
4.1 Maximum loadability tracking.....	31
4.2 Detection of Loss of the Voltage Controllability.....	32
4.3 Proposed VSL index	35
CHAPTER 5 SIMULATION RESULTS AND DISCUSSION	37
5.1 Simulation results.....	37
5.1.1 Case 1: IEEE 118-Bus system	37
5.1.2 Case 2 Hydro-Quebec network.....	43
5.1.3 Case 3: 2736-Bus system	49
5.2 Comparison to L-index	54
5.2.1 Case 1: IEEE 118-Bus system	54
5.2.2 Case 2: Hydro-Quebec network.....	56
5.2.3 Case 3: 2736-Bus system.....	58
CONCLUSION.....	61
RECOMMENDATIONS.....	63

APPENDIX I	RESULTS FOR IEEE 118-BUS SYSTEM AND HYDRO-QUEBEC NETWORK.....	65
LIST OF REFERENCES		93

LIST OF TABLES

	Page
Table 2.1	The three weakest buses of the IEEE 118-Bus system21
Table 2.2	The three strongest buses of the IEEE 118-Bus system21
Table 2.3	The three weakest buses of the Hydro-Quebec network21
Table 2.4	The three stronest buses of the Hydro-Quebec network.....22
Table 2.5	The three weakest buses of the 2736-Bus system.....22
Table 2.6	The three strongest buses of the 2736-Bus system22
Table 5.1	The three weakest buses of the IEEE 118-Bus system37
Table 5.2	The three strongest buses of the IEEE 118-Bus system38
Table 5.3	The three weakest buses of the Hydro-Quebec network43
Table 5.4	The three strongest buses of the Hydro-Quebec network.....43
Table 5.5	The three weakest buses of the 2736-Bus system.....49
Table 5.6	The three strongest buses of the 2736-Bus system49
Table 5.7	Loadability margin of the weakest buses of the IEEE 118-Bus system ...55
Table 5.8	Loadability margin of the weakest buses of the IEEE 118-Bus system55
Table 5.9	Loadability margin of the strongest buses of IEEE 118-Bus system.....56
Table 5.10	Loadability margin of the strongest buses of IEEE 118-Bus system.....56
Table 5.11	Loadability margin of the weakest buses of Hydro-Quebec network.....57
Table 5.12	Loadability margin of the weakest buses of Hydro-Quebec network.....57
Table 5.13	Loadability margin of the strongest buses of Hydro-Quebec network58
Table 5.14	Loadability margin of the strongest buses of Hydro-Quebec network58
Table 5.15	Loadability margin of the weakest buses of 2736-Bus system.....59
Table 5.16	Loadability margin of the weakest buses of 2736-Bus system.....59

Table 5.17	Loadability margin of the strongest buses of 2736-Bus system60
Table 5.18	Loadability margin of the strongest buses of 2736-Bus system60

LIST OF FIGURES

	Page
Figure 1.1 Network and load PV curves.....	9
Figure 1.2 Loss of equilibrium point due to increasing the demand	10
Figure 1.3 Voltage Controllable and Uncontrollable regions on a QV curve	11
Figure 1.4 Loss of Voltage Controllability in a constant impedance load.....	12
Figure 1.5 Simple 2-Bus system	15
Figure 1.6 PV curves for different power factors	17
Figure 3.1 Simple 2-Bus system	24
Figure 3.2 PV curve for bus 2	26
Figure 4.1 P & O algorithm to find the maximum deliverable power to bus i	32
Figure 5.1 PV curve for bus 117	39
Figure 5.2 P-VSL curve for bus 117	39
Figure 5.3 PV curve for bus 21	40
Figure 5.4 P-VSL curve for bus 21	40
Figure 5.5 PV curve for bus 68	41
Figure 5.6 P-VSL curve for bus 68	41
Figure 5.7 PV curve for bus 81	42
Figure 5.8 P-VSL curve for bus 81	42
Figure 5.9 PV curve for bus 638	45
Figure 5.10 P-VSL curve for bus 638	45
Figure 5.11 PV curve for bus 634	46
Figure 5.12 P-VSL curve for bus 634	46
Figure 5.13 PV curve for bus 141	47

Figure 5.14 P-VSL curve for bus 141	47
Figure 5.15 PV curve for bus 261	48
Figure 5.16 P-VSL curve for bus 261	48
Figure 5.17 PV curve for bus 2164	50
Figure 5.18 P-VSL curve for bus 2164	50
Figure 5.19 PV curve for bus 506	51
Figure 5.20 P-VSL curve for bus 506	51
Figure 5.21 PV curve for bus 92	52
Figure 5.22 P-VSL curve for bus 92	52
Figure 5.23 PV curve for bus 90	53
Figure 5.24 P-VSL curve for bus 90	53

LIST OF SYMBOLS AND UNITS OF MEASUREMENTS

ΔP_i	Active power variation in i^{th} bus
ΔQ_i	Reactive power variation in i^{th} bus
$\Delta \theta_i$	Voltage angle variation in i^{th} bus
ΔV_i	Voltage magnitude variation in i^{th} bus
\bar{I}^*	Conjugate of current phasor
I_{sc}^i	Short circuit current of i^{th} bus
J	Jacobian matrix
L_i	L-index of i^{th} bus
P	Active power
P_i	Initial delivered active power to i^{th} bus
P_l^k	Active power computed at k^{th} step
P_l^{k-1}	Active power computed at $(k-1)^{th}$ step
P_{mi}	Maximum loadability limit of i^{th} bus
P_{max}	Maximum of P_{mj} ($j=1, 2, \dots, n$)
P_{pu}	Active power in per unit
pu	Per unit
Q	Reactive Power
Q_{pu}	Reactive Power in per unit
R	Resistance
R_{tot}	Equivalent resistant of the total load
V	Voltage magnitude

XVIII

V_i Voltage magnitude of i^{th} bus

\bar{V}_i Voltage phasor of i^{th} bus

V_{th} Thevenin voltage

V_{nl}^i No-load voltage of i^{th} bus

X Reactance

X_l Line reactance

Y Admittance matrix

Z Impedance

Z_{th}^i Thevenin impedance seen from i^{th} bus

Z^{ii} Diagonal element of impedance matrix corresponding to i^{th} bus

Z^i Load's apparent impedance

Z_{th} Thevenin impedance

INTRODUCTION

Voltage instability refers to the continuous and uncontrollable voltage drop or rise at some buses of the system. Voltage instability may occur due to a variety of reasons. The most important factor which may lead to this phenomenon is the inability of the network to meet the reactive power demand in at least one of the buses(Taylor 1994). Voltage instability might be followed by loss of load and eventually the power system coherence.

The steep rise in demand for electrical energy in recent years has compelled power systems to operate closer to their limits than in the past(Kwatny, Pasrija et al. 1986). This makes power systems more susceptible to instances of voltage instability. If voltage instability is not addressed timely, it may eventually lead to voltage collapse(Kundur 1999). Therefore, stability analysis has become one of the top priority concerns of electric utilities. Neglecting this issue may lead to adverse economic effects. The loss caused during the August 2003 blackout in United States was estimated to be between \$4 billion and \$6 billion(Fairley 2004). Hence, utility companies need to pay considerable attention to the problem of voltage instability and should adopt effective strategies to address this issue.

Voltage stability analysis is broadly categorized into two main methods: static analysis and dynamic analysis. Dynamic methods of analysis involve the creation of time domain simulations. These models are created for each component of the system and help to track voltage fluctuations in real-time across the system. To apply dynamic analytical methods, it is necessary to perform differential equation sets. These equations embody characteristics and relationships between different electrical components in the circuit. Compared to other methods, dynamic analytical methods offer a viable opportunity to track voltage levels in real-time and take corrective action immediately. At the same time, dynamic methods are time-consuming and place considerable demands on the computer's processing capacity. Therefore, to study the large power systems, static analysis can be used(Gao, Morison et al. 1996).

In contrast to dynamic analytical methods, static methods of analysis track voltage performance at specific rather than continuous points in time. Static analysis involves a range of techniques which include modal analysis, sensitivity analysis, P-V and Q-V methods. Static analytical methods, assess voltage behaviour by deriving first or second order functions from power flow equations. These functions are then interpreted to determine whether or not and to what extent the power system can maintain stability. The functions are then processed with different values which represent specific rise levels of the load. Eventually, the researcher is able to determine the load level where voltage collapses and the system loses its stability. The maximum load level for which power system integrity is maintained is referred to as the maximum power point or maximum loadability limit. In this way, the static methods enable the identification of the maximum loadability limits for different system loading levels. Some researchers have developed voltage stability indices using static analysis methods. These indices vary for different loading conditions (from no-load to maximum power point) and reveal relatively to what extent the system is stable. Static methods are generally quite reliable because they mimic the actual behaviour of the electrical system.

Active power-Voltage (PV) curves are drawn to determine the stability margin of each bus in a network. Specific buses are selected and the loads of the selected buses are increased gradually. The power flow is performed at each step. This procedure is continued until the nose points of the PV curves are reached. The distance between the nose point of the PV curve and the current operating point of each bus is considered as the loadability margin of the bus (Canizares 2002). Depending on the load characteristics, further increase in the load would either render the power flow equations insolvable or would push the operating point to the lower portion of the PV curve and therefore the network would lose its controllability. In either case, the voltage will become unstable. Reactive power-Voltage (QV) curves are drawn to determine the loadability margin of a network. The $dQ/dV > 0$ satisfies the voltage stability condition which corresponds to the right leg of the QV curve whereas $dQ/dV < 0$ indicates the voltage instability condition which corresponds to the left leg of the QV curve (Kundur, Balu et al. 1994). Although PV and QV curves are reliable tools for voltage

stability study, generating PV and QV curves for every bus in a large network requires a long time and is hence not considered practical.

An indicator for voltage stability called L-index was proposed by (Kessel and Glavitsch 1986). The L-index is calculated for each bus on the network to identify the one with the greatest vulnerability to voltage collapse. A value of the L-index closer to unity implies that the power system is closer to the voltage instability. The L-index depicts voltage instability when the power flow equations become unsolvable. In fact, $L=1$ corresponds to the maximum loadability limit. The main drawback of the L-index is that it fails to determine the instability of the power system when the voltage becomes uncontrollable. Furthermore, the matrices for L-index calculation have to be reformed each time a PV bus hits its reactive power limits and is converted to a PQ bus.

A modal analysis approach to identify unstable buses was proposed by (Gao, Morison et al. 1992). Under the modal analysis approach, the signs of the eigenvalues of the reduced Jacobian matrix indicates voltage stability. According to the proposed modal analysis, if all the eigenvalues of the reduced Jacobian matrix are positive, it can be concluded that the network is voltage stable. Conversely, if at least one of the eigenvalues of the reduced Jacobian matrix is negative, one can conclude that the system is voltage unstable. Each negative eigenvalue of the reduced Jacobian matrix corresponds to an unstable mode in the network. The bus participation factor is calculated by using the eigenvalues and their corresponding eigenvectors. The modal analysis approach has several advantages including the evaluation of participation factor of all the network buses during voltage instability. On the other hand, its main drawback is that it does not provide a rigorous measure to specify how stable or unstable a bus is. In other words, the modal analysis approach merely indicates whether there is a voltage unstable bus in the network but does not indicate the extent to which it is unstable and which specific bus is voltage unstable.

The minimum singular value of the Jacobian matrix was proposed as an alternative approach to evaluate the voltage stability condition of a power system(Thomas and Tiranuchit 1986).

The minimum singular value is based on the singularity of the Jacobian matrix at the voltage collapse point. The distance between the minimum singular value of the decomposed Jacobian matrix and zero represents the distance from the power system at the given load condition to voltage collapse. An algorithm for calculating the minimum singular value of the Jacobian matrix was proposed by (Lof, Smed et al. 1992). The sign of the determinant of the Jacobian matrix was proposed as another indicator of voltage stability (Venikov, Stroeve et al. 1975). It was explained that under certain conditions the instability of the system can be determined from the sign of the determinant of the Jacobian matrix. A negative sign indicates that the system is unstable. Using this method as an indicator of power systems' voltage stability has some uncertainty (Tamura, Mori et al. 1983). A voltage collapse proximity indicator based on the Thevenin impedance seen at each load was proposed by (Vu, Begovic et al. 1999). However, none of these studies present an approach to identify specific buses in the system that cause the power system to be voltage unstable. Nor can these methods assess the number of such buses in the network.

This thesis proposes a novel method to determine whether a network is voltage stable or unstable. In addition, a Voltage Stability and Loadability (VSL) index is proposed which provides a rigorous measure of proximity to voltage instability for stable buses. The VSL index lies between -1 and 1. The greater the value of the VSL index, the more stable the network. The sign of the VSL index is determined by considering the controllability of the voltage. The amplitude of the VSL index is obtained by calculating the distance from the initial operating point to the maximum loadability limit of each bus. Under this approach, the loss of voltage controllability—a mechanism which causes voltage instability in a power system—is detected on the basis of the sensitivity of the power system's buses to the injection of reactive power to the same bus. In fact, a bus is said to have a stable voltage if it has positive V-Q sensitivity. On the other hand, a voltage unstable bus is identified if it has negative V-Q sensitivity. An algorithm based on Perturbation and Observation (P & O) is proposed to track the maximum loadability limit of every bus in the network. The maximum loadability limit of each bus can then be used to calculate the loadability margin of the same bus.

Objectives

During the last decades, considerable works have been done on developing methods to identify the loadability limit, and voltage stability indices. This thesis goes further to develop a method for assessing voltage stability which can be applied to networks of any size when subjected to mid-term or long-term voltage stability. Short term voltage stability is not included in the scope of this work. The sub-tasks needed to solve the problem are:

- a) computation of the maximum loadability limit under given loading condition;
- b) determination of whether or not the operating point is a voltage control operating point;
- c) compounding the results obtained from the previous two steps to define a voltage stability index which reveals a rigorous voltage stability measure.

Contributions

The findings of this thesis will make several important contributions to the field. The thesis will:

- a) develop a new technique based on simple calculations to identify unstable buses due to loss of voltage controllability in a network in much less time compared to other techniques proposed in the literature;
- b) develop a novel algorithm to reveal the loadability margin of all the load buses in a power system;
- c) develop a novel voltage stability index which provides an absolute measure of proximity to voltage instability.

Case Studies

Three different case studies are used in this thesis to test the accuracy of the proposed technique and to compare the results obtained from the VSL index as opposed to those obtained from the L-index.

Case 1: IEEE 118-Bus

The IEEE 118-Bus system consists of a total of 118 buses. Among them 64 buses are load buses, and 54 buses are voltage controlled buses. The slack bus in this network is bus 69.

Case 2: Hydro-Quebec network

Hydro-Quebec network consists of a total of 783 buses. Among them, 632 buses are load buses, and 151 buses are voltage controlled buses. There are two slack buses in this network which are buses 86 and 217.

Case 3: 2736-Bus system

This test case consists of a total of 2736 buses. Among them, 2461 buses are the load buses, and 275 buses are the voltage controlled buses. Bus 28 is the slack bus.

CHAPTER 1

VOLTAGE STABILITY

This chapter presents some concepts of voltage stability to enable the reader to understand the methods suggested for voltage stability monitoring in subsequent chapters. First, the definition of voltage stability used in this thesis is presented. Next, the mechanisms which lead to voltage instability are introduced.

1.1 Voltage stability definition

Several definitions have been proposed for voltage stability. For the purpose of the present study, the definition proposed by the IEEE Committee Report is used throughout this thesis(Committee 1990): "Voltage stability is the ability of a system to maintain voltage so that when load admittance is increased, load power will increase, and so that both power and voltage are controllable."

Several factors contribute to voltage instability. Among all other factors, the most influencing factor is the failure of power systems to meet reactive power demand in order to keep the voltage of all nodes within the viable voltage levels (Chakrabarti 2010). Nevertheless, the voltage level cannot be a reliable indicator of voltage instability (Lof, Andersson et al. 1993) because sometimes in a heavily loaded power system, it is possible that the system is in a state of voltage instability due to uncontrollability of voltage even if all the voltages lie within the normal voltage level. Generators and capacitors are the main sources of the reactive power in power systems. The inability of the power systems to meet reactive power demand may be due to limitations on production or transmission of reactive power (Abed 1999). The reactive power produced by capacitors are proportional to their voltages. Hence, low voltage levels decrease their capability to produce reactive power. On the other hand, the considerable reactive power loss on heavily loaded lines, as well as possible line failures that reduce transmission capacity, are the main limitations of reactive power transmission.

1.2 Mechanisms of voltage instability

Active and reactive power consumption of loads are both dependent on voltage magnitude and load characteristic. The load characteristic can be drawn using the static load model equations. Generally, all loads can be modelled as a combination of constant power, constant current, and constant impedance load (Tiwari and Ajjarapu 2007). The dependency of active and reactive power to the voltage magnitude and the load demand can be shown through the following equations (Cutsem and Vournas 1998):

$$P=P(V,z) \quad (1.1)$$

$$Q=Q(V,z) \quad (1.2)$$

Here, z is the load demand and its value increases or decreases directly in response to changes in demand. The load characteristic intersects with the network characteristic at two points. These two intersection points refer to the two possible solutions for voltage. Figure 1.1 illustrates the load and network characteristic.

Insolvability of the power flow equations and loss of voltage controllability are two mechanisms which cause voltage instability in power systems (Rodrigues, Prada et al. 2010).

1.2.1 Insolvability of the power flow equations

Insolvability of the power flow equations implies a situation under which at least one load violates the maximum loadability limit, and as a result the feasible equilibrium point is lost. This situation can be interpreted as follows: As the demand is increased, the load characteristic in Figure 1.1 is shifted toward the nose point of the network characteristic. For a specific amount of demand, the load characteristic becomes tangent to the network characteristic and therefore the two possible solutions of voltage coincide. This point is called the voltage collapse point. Any future increase in the demand behind the voltage collapse point results in a lack of solution for voltage. This mechanism is depicted in Figure 1.2. In other words, since there is no intersection between the load and network PV

curves, so there is no feasible equilibrium point. This mechanism is denominated as the “insolvability of the power flow equations”. During this mechanism, the stable equilibrium point disappears due to the bifurcation. The consequence of the disappeared equilibrium point is a system transient characterized by a dynamic fall of voltage which eventually leads to voltage collapse.

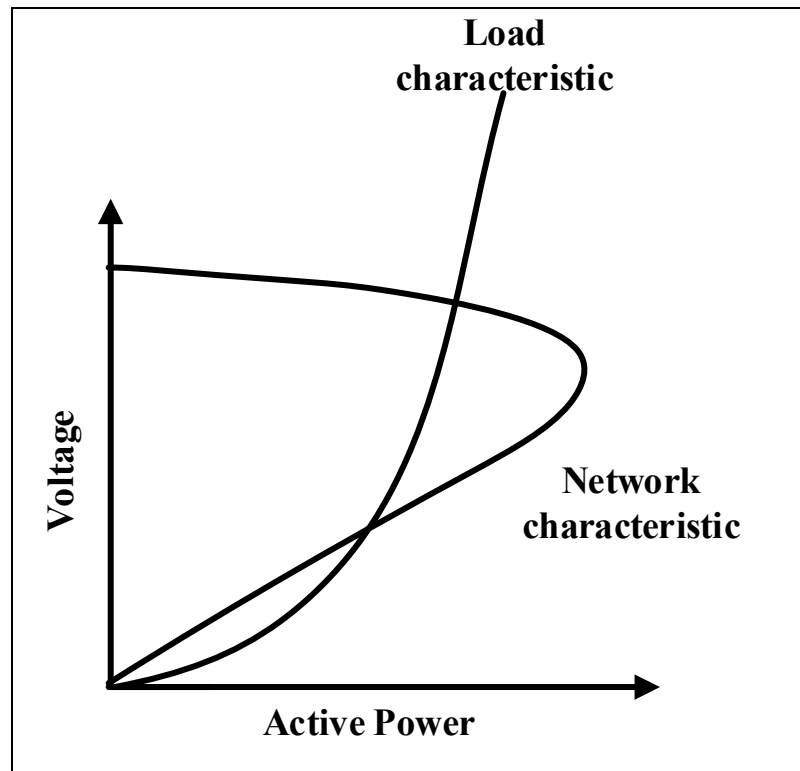


Figure 1.1 Network and load PV curves
Adopted from Cutsem and Vournas (1998)

The same scenario applies to a reactive load. When at least in one bus in the network, reactive load exceeds the maximum transferable reactive power to that bus, the equilibrium point disappears due to the violation of limit in maximum reactive power transfer. The critical point – which is the point of collapse – corresponds to the minima of the QV curve. This situation can be interpreted as the inability of power systems to supply the required reactive power in at least one bus in the network. In this case, the QV curve of the load characteristic does not intersect the QV curve of the network characteristic. The most well-

known available technique in the literature to detect how far a system is from this mechanism is the L-index.

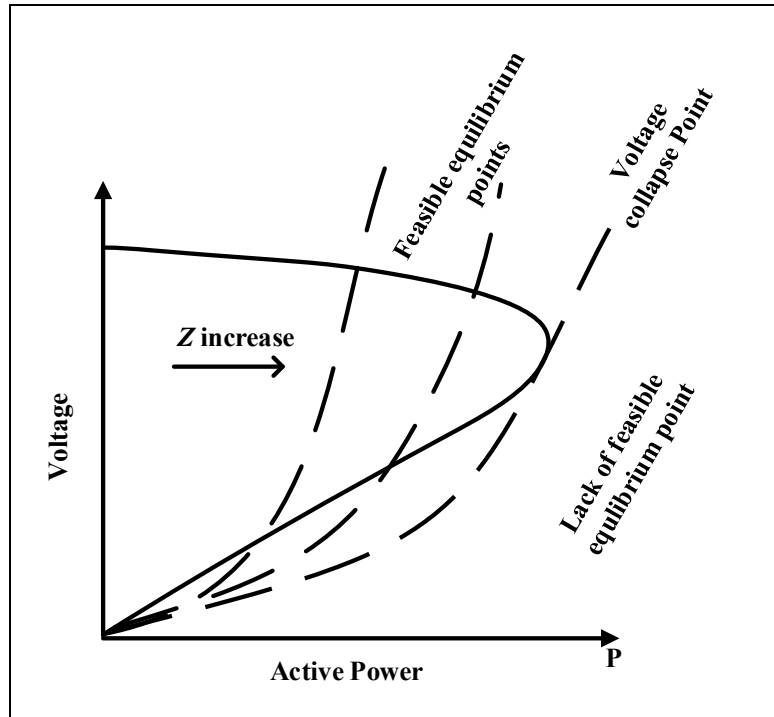


Figure 1.2 Loss of equilibrium point due to increasing the demand
Adopted from Cutsem and Vournas (1998)

1.2.2 Loss of Voltage Controllability

All the reactive power sources (Generators, SVCs, etc) that injection of reactive power at a bus will increase that bus's voltage magnitude. If this assumption is wrong, any voltage control action will result in an opposite corrective effect on the voltage magnitude of that bus. This situation is referred to as the loss of voltage controllability. The mechanism of loss of voltage controllability is directly related to the V-Q sensitivity of every bus in the system. The positive V-Q sensitivity corresponds to an equilibrium point at the right side of the QV curve. All the equilibrium points on the right side of the QV curve respond to the control actions as expected. That means that the injection of reactive power at those buses whose operating points are on this region results in a rise in their voltage magnitudes. Conversely,

injection of reactive power at those buses whose operating points are on the left side of the QV curve results in a fall in their voltage magnitudes. The V-Q sensitivity of these buses is negative and hence they are voltage uncontrollable. Figure 1.3 illustrates the voltage controllable and uncontrollable regions on a QV curve. It is to be noted that this type of instability occurs when at least a portion of load is of type constant impedance and/or constant current. Figure 1.4 illustrates this situation for a constant impedance load.

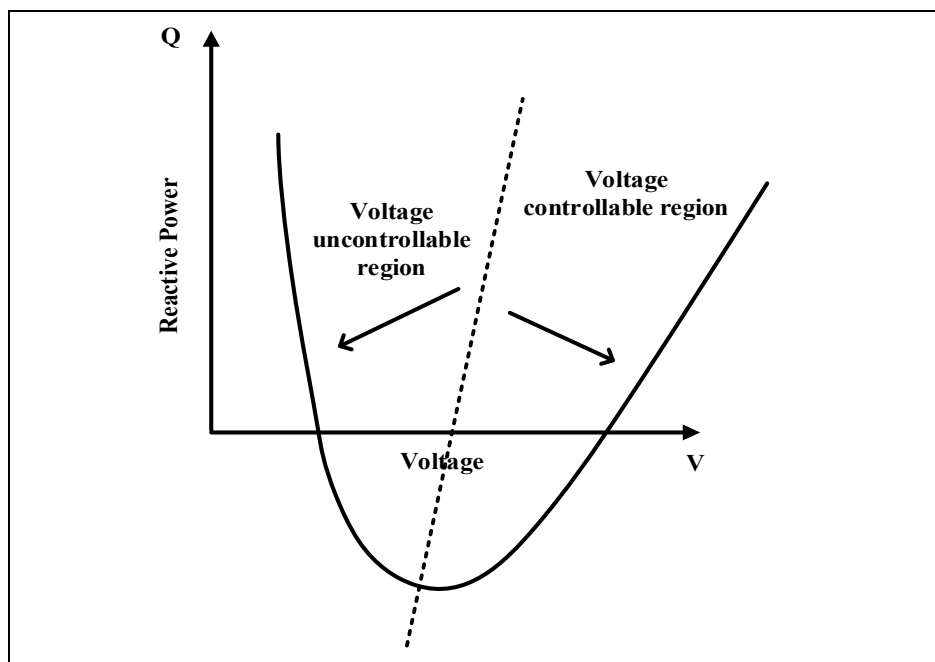


Figure 1.3 Voltage Controllable and Uncontrollable regions on a QV curve

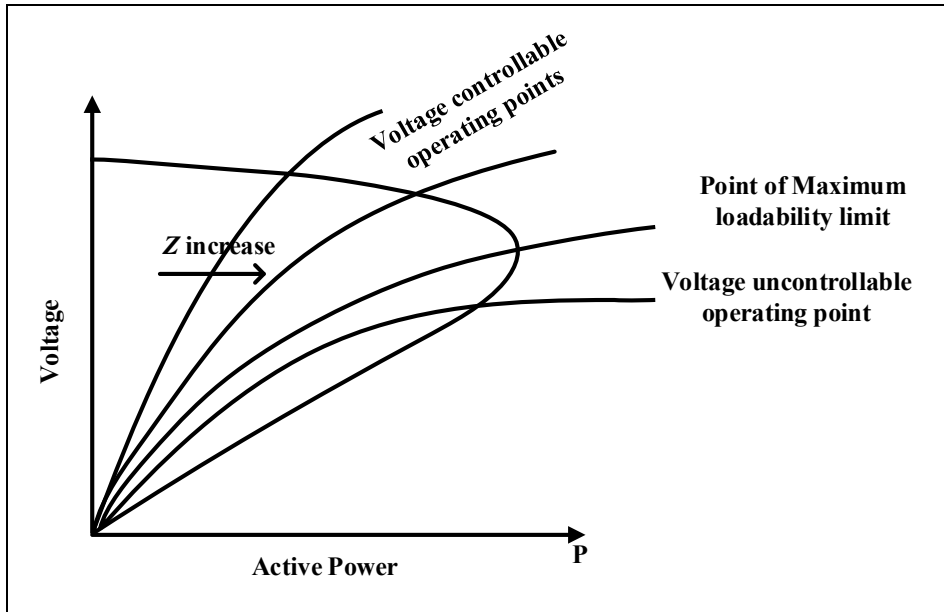


Figure 1.4 Loss of Voltage Controllability in a constant impedance load

1.3 Loadability limit vs Loadability margin

Loadability limit of a bus is the maximum power than can be delivered to the same bus. The active power value corresponding to the nose point of the PV curve is the loadability limit of the bus for which the PV curve is drawn.

Loadability margin is the distance from the current loading condition of a bus to its loadability limit.

1.4 Classification of voltage stability

The voltage instability in a power system is a consequence of a perturbation. The perturbations which cause voltage instability can be divided into short term and long term disturbances (Kundur, Paserba et al. 2004). The time span of the short term or transient voltage instability is a few seconds. The instability caused by rotor angle imbalance, loss of synchronism, and governor dynamics are some instances of short term voltage instability.

Dynamic analysis approaches should be employed to study the short term voltage instability phenomena.

The time span of the long term – also referred to as mid-term – voltage instability typically ranges in duration from ten seconds up to several minutes. This type of instability mostly occurs in heavily loaded power systems. When a power system is heavily loaded, voltage drops across the network. Voltage control equipment produce reactive power to keep the voltage profile of the power system within the viable level. This mechanism may lead to the violation of the maximum reactive power transfer limit and consequently may lead to loss of a feasible equilibrium point due to the insolvability of power flow equations.

Operators may be able to prevent the long term voltage instability by appropriate control actions such as load shedding. Static analysis approaches are effective methods to study long term voltage instability.

Static voltage stability analysis is an effective tool to study the slow mechanisms which cause voltage instability. These analysis techniques evaluate the feasibility of an equilibrium point under a specific load condition of the power system. A broad variety of power system conditions can be analysed by the static analysis approaches. The perturbations which cause long-term voltage instability are slow enough to be effectively analysed by using the static analysis approaches.

Dynamic analysis techniques are useful to study short term voltage instability. These techniques can be employed to study the causes and effects of a voltage collapse which have already occurred.

The scope of this work is to analyse voltage stability from the static point of view.

1.5 Relationship between power transfer and voltage (Mahseredjian 2012)

Estimating the maximum loadability limit of the power system load buses is one of the objectives of the Voltage stability assessment. The distance from the current operating point

of a bus to the maximum loadability limit of that bus is referred to as the loadability margin. The PV curve is one conventional solution to estimate the maximum loadability limit. In order to depict the PV curves, the load is increased step by step. Power flow is performed at each step and voltage magnitude and active power are recorded. This procedure is continued until the power flow diverges. The last value of the active power for which the power flow converges, is the maximum loadability limit.

Consider a simple 2-Bus system of Figure 1.5. For the sake of simplicity the line has been considered purely inductive ($R=0$). For the apparent power injected to bus 2 we can write:

$$S = \bar{V}_2 \bar{I}^* = \bar{V}_2 \left[\frac{\bar{V}_1 - \bar{V}_2}{jX} \right]^* = [V_2 \cos \delta - jV_2 \sin \delta] \left[\frac{V_1 - V_2 \cos \delta + jV_2 \sin \delta}{jX} \right]^* \quad (1.3)$$

The real and imaginary part of equation (1.3) are active and reactive power equations of bus 2 respectively

$$P = \frac{V_1 V_2}{X} \sin \delta \quad (1.4)$$

$$Q = \frac{V_1 V_2 \cos \delta - V_2^2}{X} \quad (1.5)$$

If the power factor of the load is $\cos \phi$, then for the voltage of bus 2 we will have:

$$V_1 = \bar{V}_2 + jX \bar{I}^* = \bar{V}_2 + jX \left[\frac{P + jQ}{\bar{V}_2} \right]^* \rightarrow V_1 \bar{V}_2^* = V_2^2 + jX[P - jQ] \quad (1.6)$$

Magnitude of I in terms of V_1 is obtained from the following equation:

$$I = \frac{V_1}{\sqrt{(Z \cos \phi)^2 + (Z \sin \phi + X)^2}} = \frac{V_1}{x \sqrt{1 + \frac{Z^2}{X^2} + 2 \frac{Z}{X} \sin \phi}} \quad (1.7)$$

And for the magnitude of V_2 we can write:

$$V_2 = ZI = \frac{Z}{X} \frac{V_1}{\sqrt{1 + \frac{Z^2}{X^2} + 2\frac{Z}{X}\sin\varphi}} \quad (1.8)$$

$$P = V_2 I \cos\varphi = ZI = \frac{Z}{X^2} \frac{V_1^2}{(1 + \frac{Z^2}{X^2} + 2\frac{Z}{X}\sin\varphi)} \cos\varphi \quad (1.9)$$

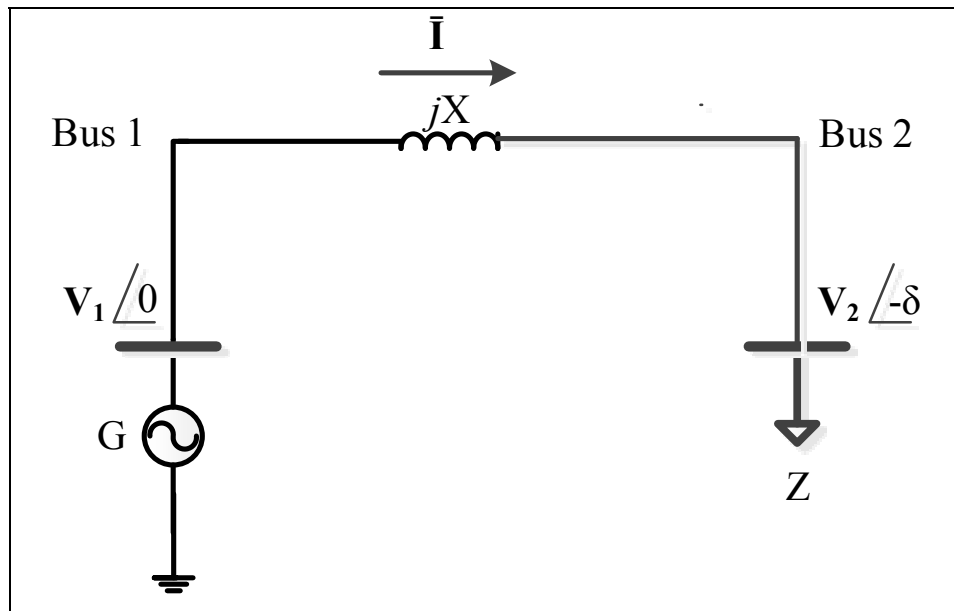


Figure 1.5 Simple 2-Bus system
Adopted from Mahseredjian (2012)

For unity power factor $\varphi = 0$

$$P = Z \frac{V_1^2}{(X^2 + Z^2)} \quad (1.10)$$

For maximum power $Z=X$

$$P_{max} = \frac{V_1^2}{2X} \quad (1.11)$$

Choosing P_{max} as P_{base} and V_1 as V_{base} equation (1.6) can be rewritten in per unit. Dividing equation (1.6) by $\frac{2X}{2X} V_1^2$ we have

$$\frac{\bar{V}_2^*}{V_1} = \frac{V_2^2}{V_1^2} + j \frac{[P - jP \tan \phi]}{2 \frac{V_1^2}{2X}} \rightarrow \bar{V}_2^*_{pu} = V_2^2_{pu} + \frac{1}{2} Q_{pu} + j \frac{1}{2} P_{pu} \quad (1.12)$$

And

$$V_2^2_{pu} = \left(V_2^2_{pu} + \frac{1}{2} Q_{pu} \right)^2 + \left(\frac{1}{2} P_{pu} \right)^2 \quad (1.13)$$

Dividing equation (1.9) by equation (1.11) gives P_{pu} as follow:

$$P_{pu} = \frac{Z}{X} \frac{2}{(1 + \frac{Z^2}{X^2} + 2 \frac{Z}{X} \sin \phi)} \cos \phi \quad (1.14)$$

The solution of equation (1.13) for different active power values and power factors is presented in Figure 1.6 (PV curves for different power factors). The QV curves can be obtained from equation (1.13). The voltage stability limits are obtained when the differential of Q against V_2 becomes zero. The points on the left side of the QV curves are unstable points. The system is stable in the region

$$\frac{\partial Q}{\partial V_2} > 0 \quad (1.15)$$

The voltage stability limit is reached when the differential is zero.

There are two equations proposed in the literature for the loadability margin of a power system with n load buses as follows:

$$LM_i = \frac{P_{mi} - P_i}{P_{mi}} \quad (1.16)$$

$$LM_i = \frac{P_{mi} - P_i}{P_{max}} \quad (1.17)$$

Where

LM_i is the loadability margin of bus i

P_{mi} is the deliverable active power to bus i corresponding to the nose point on the PV curve (maximum loadability limit)

P_i is the delivered active power to bus i at the time of computing the loadability margin.

P_{max} is the maximum of P_{mj} ($j = 1, 2, \dots, n$)

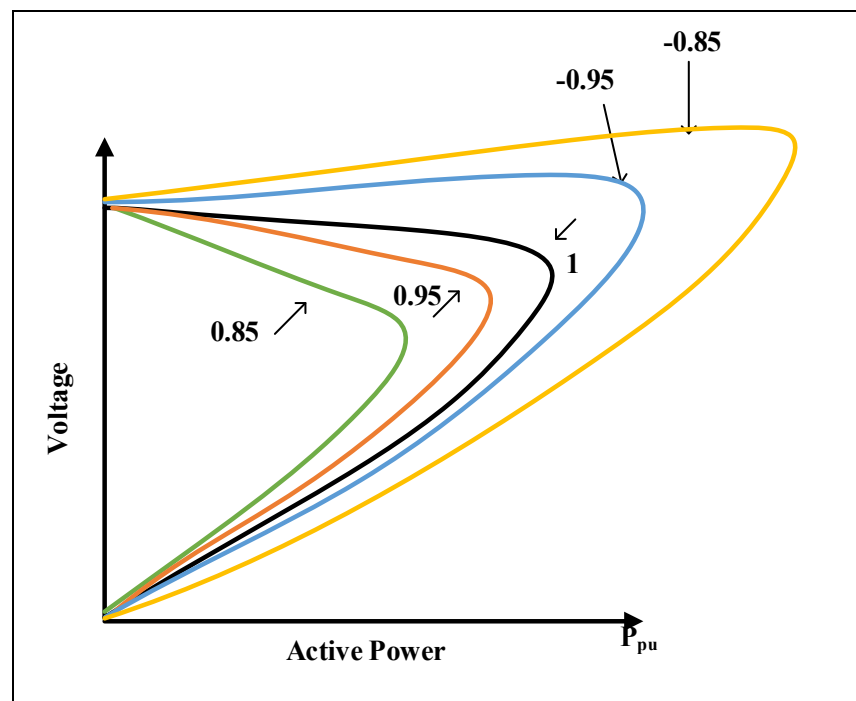


Figure 1.6 PV curves for different power factors
Adopted from Mahseredjian (2012)

The loadability margin can be expressed as a percentage. In this case, the values obtained from equation (1.16) and (1.17) should be multiplied by 100. The bus having the maximum LM is considered to be the strongest bus, and conversely the bus having the minimum LM is considered the weakest bus. The following example shows that equation 1.17 provides more accurate expression than equation 1.16 for the loadability margin:

Bus 1: $P_1 = 0.1 \text{ pu}$ $P_{m1} = 1 \text{ pu}$

Bus 2: $P_2 = 1 \text{ pu}$ $P_{m2} = 10 \text{ pu}$

$$P_{max} = 20 \text{ pu}$$

According to equation 1.16:

$$LM_1 = \frac{P_{m1} - P_1}{P_{m1}} \rightarrow LM_i = \frac{1 - 0.1}{1} = 0.9$$

$$LM_2 = \frac{P_{m2} - P_2}{P_{m2}} \rightarrow LM_i = \frac{10 - 1}{10} = 0.9$$

According to equation 1.17:

$$LM_1 = \frac{P_{m1} - P_1}{P_{max}} \rightarrow LM_i = \frac{1 - 0.1}{20} = 0.045$$

$$LM_2 = \frac{P_{m2} - P_2}{P_{max}} \rightarrow LM_i = \frac{10 - 1}{20} = 0.45$$

The result obtained from equation 1.17 makes more sense because despite the result obtained from equation 1.16 which suggests buses 1 and 2 have the same loadability margin, bus 2 can be loaded 10 times more than bus 1 before reaching its maximum loadability limit.

In this thesis, wherever the term “loadability margin” is used, it refers to the loadability margin which is obtained from equation 1.17.

CHAPTER 2

L-INDEX

In this chapter, the L-index – which is the most well-known voltage stability index – is briefly described. This index is then applied to three different test cases and simulation results are presented. The results obtained in this chapter will be discussed and compared to the results obtained by VSL index in chapter 5.

Kessel and Glavitsch(Kessel and Glavitsch 1986) proposed an index to assess the stability status of the load buses in a power system. L-index lies between 0 and 1. An L-index equal to 0 implies a no-load condition, whereas an L-index equal to 1 implies a voltage collapse point. This index is computed for all the load buses in a network and the greatest value obtained for L is considered to be the L-index of the network. The weakest bus of the power system is the bus whose L-index is greater than the L-index of other buses. Therefore the value of 1-L can be considered as the loadability margin of the load buses.

For a power system with the number of generator buses equal to g and the number of the load buses equal to L, at a given operating condition, the L-index is computed from the following equation:

$$L_i = \left| 1 - \sum_{j=1}^m F_{ij} \frac{V_j}{V_i} \right| \quad (2.1)$$

Where:

j : Represents any generator bus in the system $i=1, \dots, g$.

i : Represents any load bus in the system $j=m+1, \dots, L$.

V_j : Represents the voltage as a complex value at a generator bus number j .

V_i : Represents the voltage as a complex value at a load bus number i .

F_{ij} : Is a matrix with dimension $j \times i$ which is derived from the Y bus matrix

To obtain the F matrix, one should rearrange the Y matrix as follow:

$$\begin{bmatrix} I_G \\ I_L \end{bmatrix} = \begin{bmatrix} Y_{GG} & Y_{GL} \\ Y_{LG} & Y_{LL} \end{bmatrix} \begin{bmatrix} V_G \\ V_L \end{bmatrix} \quad (2.2)$$

Where:

I_G , I_L and V_G , V_L : represent currents and voltages at the generator and load buses .

The matrix F is obtained from the following relation:

$$[F]_{ji} = -Y_{LL}^{-1} Y_{LG} \quad (2.3)$$

A maximum value of L less than one satisfies the voltage stability condition of the network. The power systems having an L-index close to 1 are prone to voltage instability. As it was pointed out in chapter 1 of the thesis, the main drawback of the L-index is that this technique fails to detect the voltage instability which occurred due to the uncontrollability of the voltage.

The results of the simulation of three different test cases are presented in this section. The results will be discussed later on, in chapter 5.

2.1 Simulation Results

L-index technique was applied to three different case studies. The test results are presented in this section.

2.1.1 Case 1: IEEE 118-Bus

L-indices of all the load buses were calculated. The three weakest buses and the three strongest buses based on their L-indices are tabulated in Table 2.1 and Table 2.2 respectively. According to the L-indices, the weakest bus of the IEEE 118-Bus system is bus 44. Buses 45 and 95 are the two next weakest buses of this system. The second and third column of all the tables of this chapter, show the active and reactive power consumption of the connected loads to the corresponding buses under the given loading condition.

Table 2.1 The three weakest buses of IEEE 118-Bus system

Bus number	Active power	Reactive power	L-index
44	0.16	0.08	0.069
45	0.53	0.22	0.059
95	0.42	0.31	0.053

According to the L-indices, the strongest buses of the IEEE 118-Bus system are buses 68, 71, and 63. The value of the L-index for all these buses is 0 therefore they have the same level of strength.

Table 2.2 The three strongest buses of IEEE 118-Bus system

Bus number	Active power	Reactive power	L-index
68	39.472	1	0
71	12.1087	0.3068	0
63	20.5875	0.5216	0

2.1.2 Case 2: Hydro-Quebec network

L-indices of all the load buses were calculated. The three weakest buses and the three strongest buses based on their L-indices are presented in Table 2.3 and Table 2.4 respectively.

Table 2.3 The three weakest buses of Hydro-Quebec network

Bus number	Active power	Reactive power	L-index
638	0.645	0.147	0.976
634	0	0	0.959
678	1.002	0.261	0.924

L-indices of the Hydro-Quebec network suggest that the weakest bus is bus 638. Buses 634, and 678 are the two next weakest buses of this network.

Buses 64, 65 and 146 are the three buses in this network whose L-indices are 0, indicating that these three buses are commonly the strongest buses of the network.

Table 2.4 The three stronest buses of Hydro-Quebec network

Bus number	Active power	Reactive power	L-index
64	0	0	0
65	0	0	0
146	0	0	0

2.1.3 Case 3: 2736-Bus system

L-indices of all load buses were calculated. The three weakest buses and the three strongest buses based on their L-indices are presented in Table 2.5 and Table 2.6 respectively.

Table 2.5 The three weakest buses of 2736-Bus system

Bus number	Active power	Reactive power	L-index
506	3.197	1.000	0.179
260	4.795	0	0.173
250	2.664	0.500	0.165

Table 2.6 The three strongest buses of 2736-Bus system

Bus number	Active power	Reactive power	L-index
1963	0	0	0
1992	0	0	0
1998	0	0	0

CHAPTER 3

RELATIONSHIP BETWEEN THE MAXIMUM LOADABILITY AND THEVENIN IMPEDANCE

The power delivered to a bus is inversely proportional to the apparent impedance of the load connected to that bus. At no-load condition ($P=0$), the load's apparent impedance is infinity. As the apparent impedance decreases, the injected power is increased. Decreasing the load's apparent impedance is identical to increasing its load. When the load's apparent impedance and the Thevenin impedance seen from that load are identical to each other in magnitude, the maximum power is transferred to that load. This famous result is termed the Maximum Power Transfer Theorem. Depending on the load characteristic (Constant impedance, constant current, constant power, etc.) further decrease in the magnitude of the load's apparent impedance (in other words, further increase in the load's demand), results in either a decrease in injected power to that bus, or the disappearance of the operating point due to insolvability of the power flow equations. In both conditions, the system will undergo the voltage instability condition. In this chapter, the relationship between the power transfer and load impedance is discussed.

3.1 Relationship between PV curve and load's apparent impedance

Consider a simple 2-bus system of Figure 3.1. In this figure, bus 1 is the generator bus (PV) and bus 2 is the load bus (PQ). For the sake of simplicity, the load is assumed to be purely resistive. As can be seen in the figure, several loads have been connected to bus 2 in parallel. According to Figure 3.1:

$$V_R = \frac{V_S}{(R_{tot} + jX_L)} R_{tot} \quad (3.1)$$

Where:

V_R : phasor voltage of Bus 2

V_S : phasor voltage of Bus 1

R_{tot} : equivalent resistant of the total load

X_l : line reactance

The active power delivered to Bus 2 is

$$P_R = \frac{|V_R|^2}{R_{tot}} \quad (3.2)$$

P_R : active power delivered to Bus 2

$|V_R|$: voltage magnitude of Bus 2

Substituting equation (3.1) in (3.2) gives:

$$P_R = \frac{|V_S|^2}{R_{tot}^2 + X_l^2} R_{tot} \quad (3.3)$$

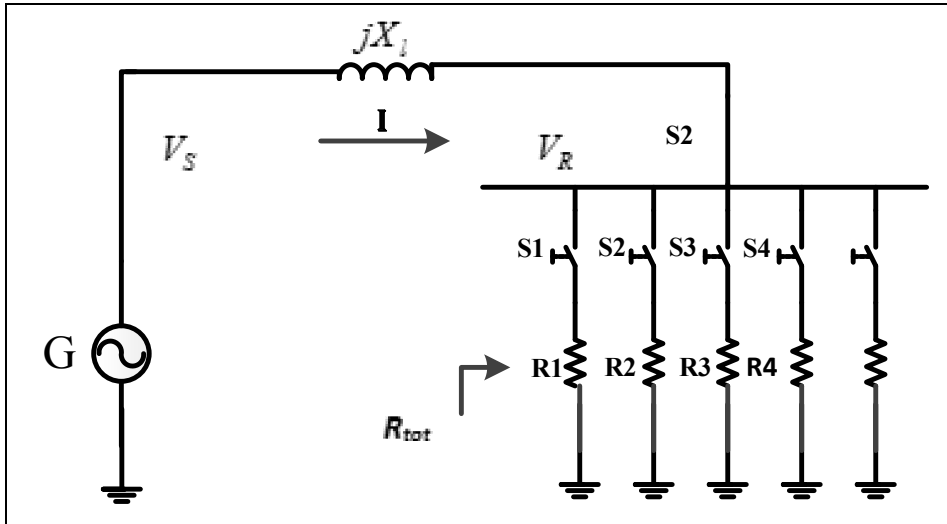


Figure 3.1 Simple 2-Bus system

Suppose that V_S is controlled to remain constant. As the demand is increased by switching on S1, S2, S3, S4 and S5 consecutively, R_{tot} is consequently decreased. As R_{tot} is decreased, the delivered active power to bus 2 increases. In other words, the delivered power to bus 2 is

inversely proportional to the value of R_{tot} . This relationship between the delivered active power and the load impedance is as expected. So, as far as decreasing R_{tot} results in increasing the delivered active power, the network is operating under normal conditions. The relationship between the delivered active power to bus 2 and R_{tot} is not always inversely proportional – rather, there is a specific value of R_{tot} behind which, the relationship between those two parameters becomes directly proportional. Figure 7 illustrates PV curve of Bus 2. In this figure:

$$P_1 = P_R|_{R_{tot}=R_1}$$

$$P_2 = P_R|_{R_{tot}=R_1||R_2}$$

$$P_3 = P_R|_{R_{tot}=R_1||R_2||R_3} = P_R|_{R_{tot}=R_1||R_2||R_3||R_4||R_5}$$

$$P_4 = P_R|_{R_{tot}=R_1||R_2||R_3||R_4}$$

$$P_{cr} = P_R|_{R_{tot}=R_{cr}}$$

R_{cr} is the value of resistant for which maximum power is delivered to Bus 2. P_{cr} represents the maximum loadability limit of Bus 2. To obtain the value of R_{cr} , one must obtain the derivative of P_R with respect to R_{tot} . A negative sign of the derivative of P_R with respect to R_{tot} means that there is a positive correlation between them: a decrease in R_{tot} results in an increase in P_R (higher portion of the PV curve). On the contrary, a positive sign of the derivative of P_R with respect to R_{tot} means that there is a negative correlation between P_R and R_{tot} : a decrease in R_{tot} results in a decrease of P_R as well (lower portion of the PV curve).

$$\frac{dP_R}{dR_{tot}} = \frac{d}{dR_{tot}} \left(\frac{|V_S|^2}{R_{tot}^2 + X_l^2} R_{tot} \right) = \left(\frac{|V_S|(X_l^2 - R_{tot}^2)}{(R_{tot}^2 + X_l^2)^2} \right) \quad (3.4)$$

For the higher portion of the PV curve:

$$\frac{dP_R}{dR_{th}} < 0 \rightarrow R_{tot} > X_l \quad (3.5)$$

For the lower portion of the PV curve:

$$\frac{dP_R}{dR_{th}} > 0 \rightarrow R_{tot} < X_l \quad (3.6)$$

For the nose point of the PV curve that corresponds to P_{cr}

$$\frac{dP_R}{dR_{th}} = 0 \rightarrow R_{tot} = R_{cr} = X_l \quad (3.7)$$

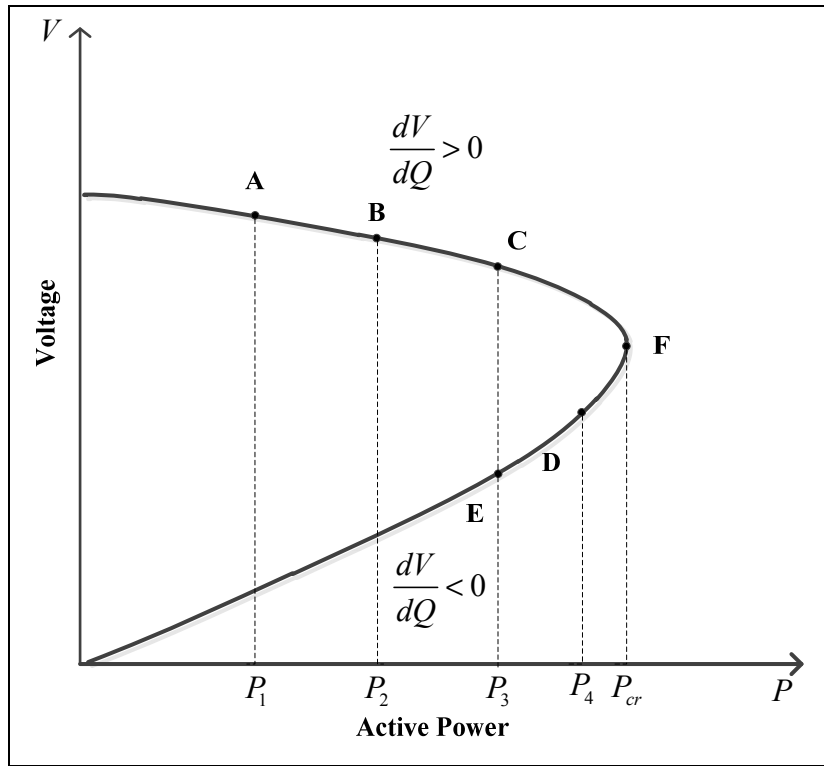


Figure3.2 PV curve for bus 2

When the equilibrium point of a load is at the higher portion of the PV curve (equilibrium points A, B and C), injection of reactive power would increase the voltage magnitude. On the contrary, when the equilibrium point of a load is at the lower portion of the PV curve (equilibrium points D and E), injection of reactive power would decrease the voltage magnitude (Lagace 2012). When the equilibrium point of a load is at the nose point of the PV

curve (equilibrium point F), injection of reactive power would not result in any variation in the voltage magnitude ($\frac{dV}{dQ} = 0$). The nose point is considered to be the point of voltage collapse or the point of maximum loadability. The equilibrium points at the higher portion of the PV curve are voltage controllable, and the equilibrium points at the lower portion of the PV are voltage uncontrollable. Those equilibrium points belong to the lower portion of the PV curve, and are voltage unstable because any corrective action of the voltage control equipment has a negative corrective effect on them.

Diagnosing whether or not the system is operating under a voltage stable condition in order to adopt appropriate control strategies, is very important. The onset of a voltage instability is not always accompanied by a significant voltage drop. However, it could eventually cause a voltage collapse in the entire power system. Even if the voltages of the unstable buses (due to voltage uncontrollability) are viable, treating them the same as the stable buses would lead to worsening the condition of voltage stability of the system. This is due to the fact that injection of reactive power at unstable buses would decrease their voltages.

3.2 Generalization to n-bus system

According to the circuit theory, any arbitrary network composed of n buses can be represented by a voltage source (V_{th}) and an impedance (Z_{th}). If in the two-bus system, we replace generator of bus 1 by V_{th} and also replace line impedance by Z_{th} , all the conclusions driven for the two-bus system will remain valid. This means, for $|Z_l| > |Z_{th}|$, the equilibrium point is on the higher portion of the PV curve and thus the system is voltage stable. On the contrary, for $|Z_l| < |Z_{th}|$ the equilibrium point is on the lower portion of the PV curve and thus the system is voltage unstable. Maximum active power deliverable to any specific bus can be easily calculated, provided that the magnitude of Z_{th} is known. Calculating Z_{th} is not complicated for the linear networks. For the linear networks V_{th} of each bus is equal to the no-load voltage of the same bus, and Z_{th} seen from each bus is computed by dividing the no-load voltage by the short circuit current of the same bus.

$$Z_{th}^i = \frac{V_{nl}^i}{I_{sc}^i} \quad (3.8)$$

Where V_{nl}^i is the no-load voltage of bus i and I_{sc}^i is the short circuit current of bus i . It is to be noted that in linear networks for all buses $V_{nl}=V_{th}$.

Calculating Z_{th} for power systems with nonlinear loads and elements is complicated. In the linear electrical circuits, Z_{th} seen from each node is its corresponding diagonal element of Z matrix. For example, in a 3 bus circuit the Thevenin impedance seen from the bus 3 is the last diagonal element of its Impedance matrix. It is to be noted that Z_{th} obtained from the Z matrix includes impedance of the bus where Z_{th} has been obtained, thus the exact Z_{th} seen from bus i^{th} is calculated as follow:

$$\frac{Z_{th}^i * Z^i}{Z_{th}^i + Z^i} = Z^{ii} \rightarrow Z_{th}^i = \frac{(Z_{th}^i + Z^i) * Z^{ii}}{Z^i} \rightarrow Z_{th}^i = \frac{Z^i * Z^{ii}}{Z^i - Z^{ii}} \quad (3.9)$$

Where:

Z_{th}^i is Z_{th} seen from bus i^{th}

Z^{ii} is the diagonal element of Z matrix corresponding to bus i^{th}

Z^i is the load's apparent impedance and is calculated from the following equation:

$$Z^i = \frac{VV^*}{S^*} \quad (3.10)$$

Where V , V^* and S^* are complex numbers and represent voltage, voltage conjugate and apparent power conjugate of i^{th} bus respectively.

Z_{th} obtained from this method is utilized later on in this thesis to estimate maximum deliverable active power to all the load buses of a power system. As it is mentioned earlier, this method to obtain Z_{th} is valid for linear electrical circuits. Thus, since power systems are a

nonlinear circuit, another approach is required to calculate Z_{th} . In this thesis, a Perturbation & Observation (P & O) algorithm is utilized to calculate Z_{th} .

CHAPTER 4

PROPOSED VOLTAGE STABILITY ASSESSMENT TECHNIQUE

In this chapter, the proposed VSL index is presented. First, the P&O algorithm is employed to obtain the maximum loadability of each bus. The voltage controllability of each bus is then examined using a V-Q sensitivity analysis.

4.1 Maximum loadability tracking

The P&O algorithm is the most popular approach to track the maximum power point in photovoltaic systems. It operates by periodically perturbing (i.e. incrementing or decrementing) the array terminal voltage and comparing the PV output power with that of the previous perturbation cycle. If the power is increasing, the perturbation will continue in the same direction in the next cycle, otherwise the perturbation direction will be reversed (Hussein, Muta et al. 1995).

In this thesis the P & O algorithm is used to obtain maximum loadability of all the load buses in a power system. As it was discussed in chapter 3, maximum loadability of any bus is reached when the magnitude of its apparent impedance is equal to the magnitude of the Thevenin impedance seen from the same bus.

P & O algorithm to find the maximum deliverable power to bus i is shown in figure 4.1.

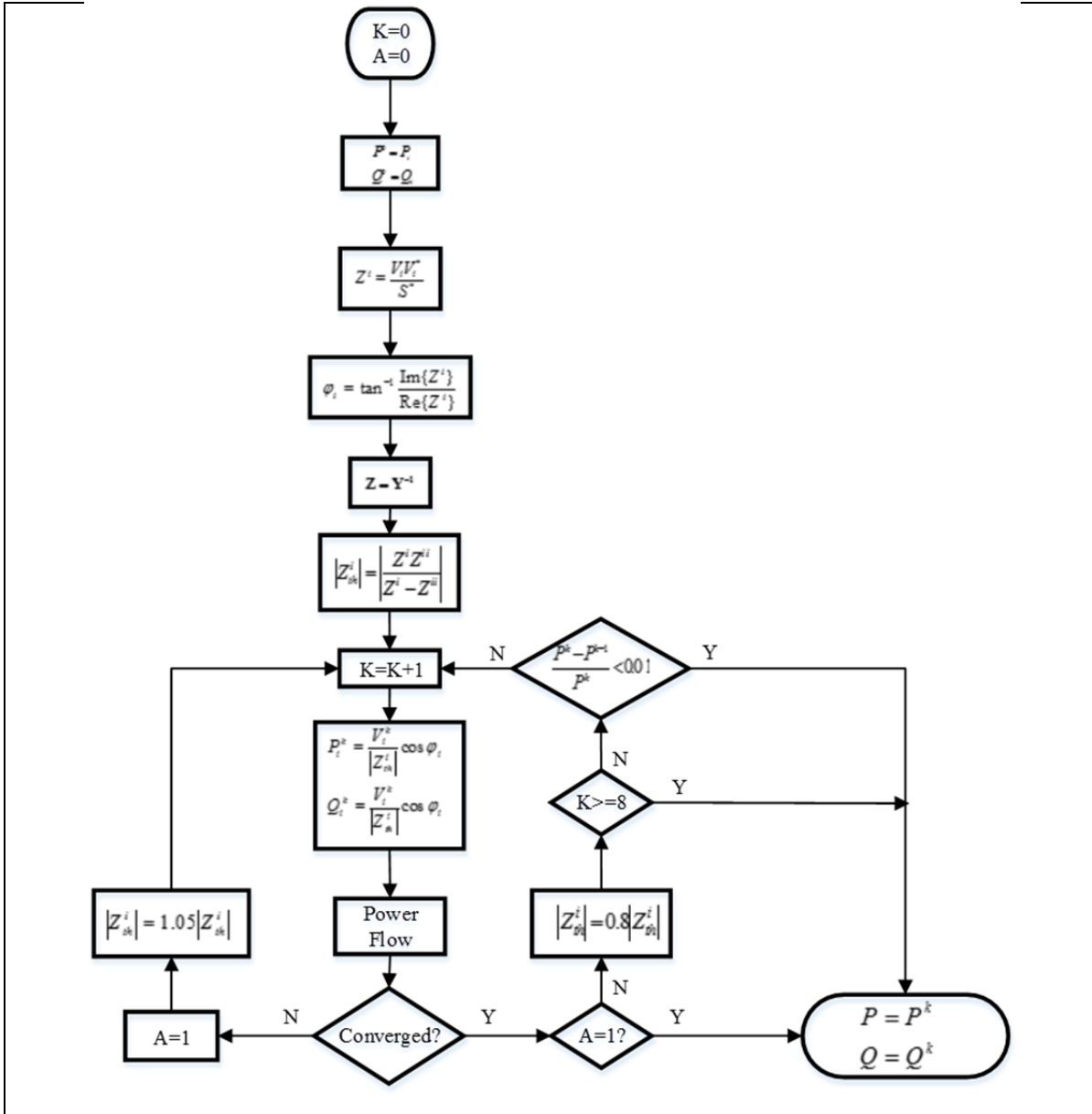


Figure 4.1 P & O algorithm to find the maximum deliverable power to bus i

4.2 Detection of Loss of the Voltage Controllability

All voltage control systems (transformer taps, SVCs, shunt capacitors, generators, etc...) assume that injection of reactive power (Q) would increase Voltage magnitude (V). If this assumption is wrong, then the control systems would behave incorrectly by having the opposite effect on the voltage magnitude. QV relationship determines the sensitivity and variation of the bus voltages with respect to the reactive power injections or absorptions. “A

system is voltage stable if V-Q sensitivity is positive for every bus, and voltage unstable if V-Q sensitivity is negative for at least one bus”(Gao, Morison et al. 1992). In other words, if the voltage of a bus is diminished following an injection of reactive power to that bus, one can conclude that the bus is voltage uncontrollable and hence voltage unstable. Therefore, if the voltage profile of the power system followed by an injection of reactive power to every bus, one by one, is predicted and compared with the current voltage profile of the same bus, the voltage stability condition of each bus is revealed. In order to be more clarified, suppose that a fictitious capacitor is connected to all the buses of the power system; at a moment of time all the fictitious capacitors are off except the fictitious capacitor located at the i^{th} bus. If the voltage variation of the i^{th} bus is positive, one can conclude that the bus is voltage stable. Otherwise, the bus is voltage unstable. Therefore, if we can predict the reaction of the voltage of each bus with respect to injection of reactive power to the bus, then we can identify whether or not the bus is voltage stable.

The Jacobian matrix is employed in Newton-Raphson method to solve power flow problems. At each iteration of the Newton-Raphson method, voltage and angle variations obtained from the previous iteration are used to calculate the active and reactive power variations. The Jacobian matrix relates the angle and voltage variations to the active and reactive power variations. Therefore, using the inverse of the Jacobian matrix, angle and voltage variations due to a slight injection of reactive power can be predicted.

The elements of the Jacobian matrix are calculated from the solved power flow. If the sign of the voltage magnitude variation of the bus corresponding to a positive reactive power variation is negative, one can conclude that the bus is operating in an unstable equilibrium point.

The relationship between the Jacobian matrix, the net injected active and reactive power variation and the voltage magnitude and angle variation is as follows:

$$\begin{bmatrix} \Delta P_2 \\ \vdots \\ \Delta P_n \\ \Delta Q_2 \\ \vdots \\ \Delta Q_m \end{bmatrix} = \begin{bmatrix} \frac{\partial P_2}{\partial \theta_2} & \dots & \frac{\partial P_2}{\partial \theta_n} & \frac{\partial P_2}{\partial V_2} & \dots & \frac{\partial P_2}{\partial V_n} \\ \vdots & \ddots & \vdots & \vdots & \ddots & \vdots \\ \frac{\partial P_n}{\partial \theta_2} & \dots & \frac{\partial P_n}{\partial \theta_n} & \frac{\partial P_n}{\partial V_2} & \dots & \frac{\partial P_n}{\partial V_n} \\ \frac{\partial Q_2}{\partial \theta_2} & \dots & \frac{\partial Q_2}{\partial \theta_n} & \frac{\partial Q_2}{\partial V_2} & \dots & \frac{\partial Q_2}{\partial V_n} \\ \vdots & \ddots & \vdots & \vdots & \ddots & \vdots \\ \frac{\partial Q_m}{\partial \theta_2} & \dots & \frac{\partial Q_m}{\partial \theta_n} & \frac{\partial Q_m}{\partial V_2} & \dots & \frac{\partial Q_m}{\partial V_n} \end{bmatrix} \begin{bmatrix} \Delta \theta_2 \\ \vdots \\ \Delta \theta_n \\ \Delta V_2 \\ \vdots \\ \Delta V_m \end{bmatrix} \quad (4.3)$$

Where:

$\Delta P_2, \dots, \Delta P_n$ = variation in the i^{th} bus active power

$\Delta Q_2, \dots, \Delta Q_m$ = variation in the i^{th} bus reactive power

$\Delta \theta_2, \dots, \Delta \theta_n$ = variation in the i^{th} bus voltage angle

$\Delta V_2, \dots, \Delta V_m$ = variation in the i^{th} bus voltage magnitude

n = number of the network buses

m = number of load buses

Rewriting equation (4.3) in terms of $\Delta \theta$ and ΔV gives:

$$\begin{bmatrix} \Delta \theta_2 \\ \vdots \\ \Delta \theta_n \\ \Delta V_2 \\ \vdots \\ \Delta V_n \end{bmatrix} = J^{-1} \begin{bmatrix} \Delta P_2 \\ \vdots \\ \Delta P_n \\ \Delta Q_2 \\ \vdots \\ \Delta Q_m \end{bmatrix} \quad (4.4)$$

Where:

J^{-1} = inverse of the Jacobian matrix.

Equation (4.4) can be rewritten as follow:

$$\begin{bmatrix} \Delta \theta \\ \Delta V \end{bmatrix} = \begin{bmatrix} A_{11} & A_{12} \\ A_{21} & A_{22} \end{bmatrix} \begin{bmatrix} \Delta P \\ \Delta Q \end{bmatrix} \quad (4.5)$$

From the equation (4.5), one can obviously conclude that if a particular amount of reactive power is injected at every bus of the network, the voltage of the same bus is varied along the sign of the corresponding diagonal element of A_{22} . In other words, negative signs of the diagonal elements of A_{22} correspond to voltage unstable buses of the network.

4.3 Proposed VSL index

An algorithm to track maximum loadability of every bus in power systems was proposed in the second section of this chapter. Additionally, an approach to find the voltage uncontrollable buses was proposed in the third section of this chapter. Now, we use the results of the two previous sections to propose a novel index for evaluating stability condition of the power systems.

In a power system with n load bus, the VSL index of the i^{th} bus is obtained from the following equation:

$$VSL_i = \text{sign}(A_{22ii}) \frac{P_{mi} - P_i}{P_{max}} \quad (4.6)$$

Where:

P_{mi} is the maximum power deliverable to bus i

P_i is the current active power of bus i

P_{max} is the maximum of $P_{mk} (k = 1, 2, \dots, n)$

$\text{sign}(A_{22ii})$ is the sign of the ii^{th} element of the sub matrix A_{22} in relationship (4.5)

The VSL indices lie between -1 and 1. The bus having a VSL index of 1 has the best stability condition and the bus having a VSL index of -1 implies the worst stability condition. As the VSL index of a specific bus decreases from 1 to 0, the corresponding bus becomes more vulnerable to voltage collapse. When the injected power to a bus is equal to its maximum deliverable power, the numerator of the equation 4.6 becomes zero. Therefore, the VSL index of 0 implies to the nose point of PV curve.

CHAPTER 5

SIMULATION RESULTS AND DISCUSSION

In this chapter, results of applying the VSL technique to the case studies are presented. The results are then compared to those of obtained from L-index.

5.1 Simulation results

5.1.1 Case 1: IEEE 118-Bus system

Maximum loadability limit of all the load buses of IEEE 118-Bus system were obtained by the P&O algorithm. It was found that bus 68 has the maximum loadability limit, and its amount is 38.576 pu ($S_b=100\text{MVA}$). Bus 21 has the minimum loadability limit. Its amount is 1.967 pu.

The three weakest and three strongest buses of the IEEE 118-Bus system are illustrated in tables 5.1 and 5.2 respectively.

Table 5.1 The three weakest buses of IEEE 118-Bus system

Bus number	P_i (pu)	Q_i (pu)	P_{mi} (pu)	Q_{mi} (pu)	VSL
117	0.2	0.08	2.001	0.799	0.047
21	0.14	0.08	1.967	1.124	0.048
44	0.16	0.08	2.038	1.018	0.048

To validate the results, we chose two buses from each table and plotted the PV curves as well as the VSL index with respect to the variation in injected active power for those buses.

To validate the results, we chose two buses from each table and plotted the PV curves as well as the VSL index with respect to the variation in injected active power for those buses.

As it can be seen in Figure 5.1 as delivered active power to bus 117 is increased from 0.2 pu to about 2 pu which is the nose point of the PV curve, the VSL decreases from 0.047 to 0. It is clear that a VSL of zero corresponds to the nose point of the PV curve. As soon as the equilibrium point reaches the voltage unstable region – i.e the lower portion of the PV curve – the VSL becomes negative. As the load gets heavier, the injected active power at bus 117 decreases and at the same time, the magnitude of the VSL increases but with a negative sign (Figure 5.2). As the VSL moves from 0 to -1, the voltage stability worsens.

Figure 5.3 illustrates the PV curve for bus 21. According to Figure 5.3, increasing the active power delivered to bus 21 from 0.14 pu to 1.967 pu, results in decreasing its VSL index from 0.048 to 0. Moving the operating point from the upper portion of the PV curve to the lower portion is concurrent to changing the sign of the VSL index from positive to negative (Figure 5.4).

Table 5.2 The three strongest buses of IEEE 118-Bus system

Bus number	P_i (pu)	Q_i (pu)	P_{mi} (pu)	Q_{mi} (pu)	VSL
68	0	0	38.376	0	1
81	0	0	31.589	0	0.824
64	0	0	27.430	0	0.715

According to the VSL indices of the load buses of the IEEE 118-Bus system, bus 68 is the strongest bus of the system. Figures 5.5 and 5.6 illustrate the PV and the VSL-Active Power curves for bus 68 respectively.

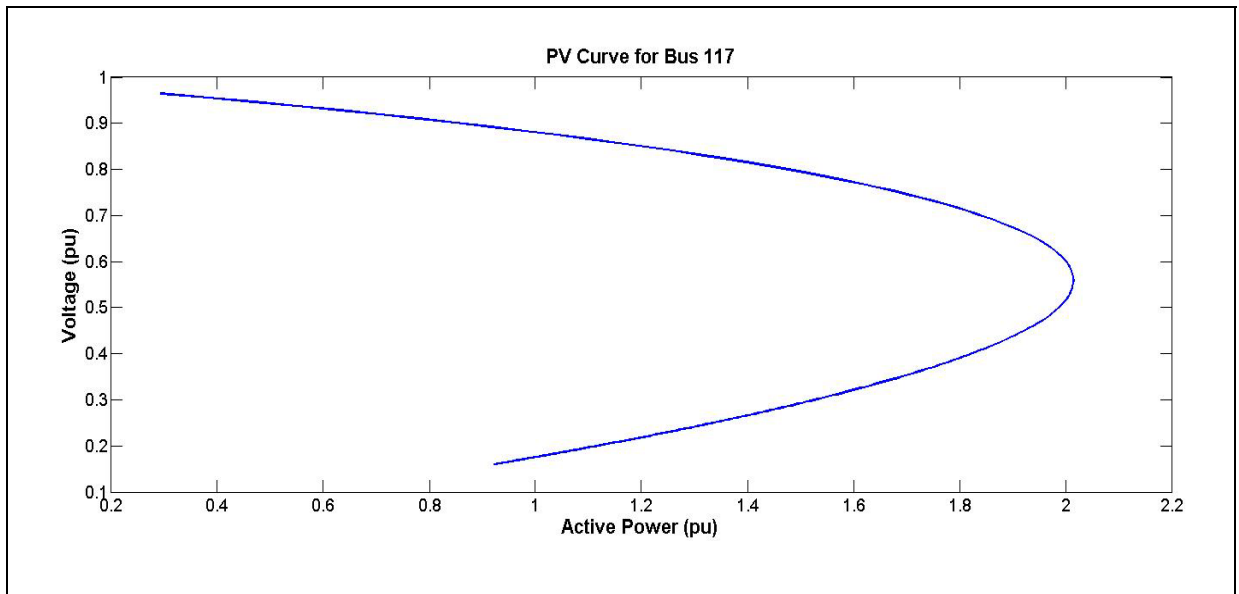


Figure 5.1 PV curve for bus 117

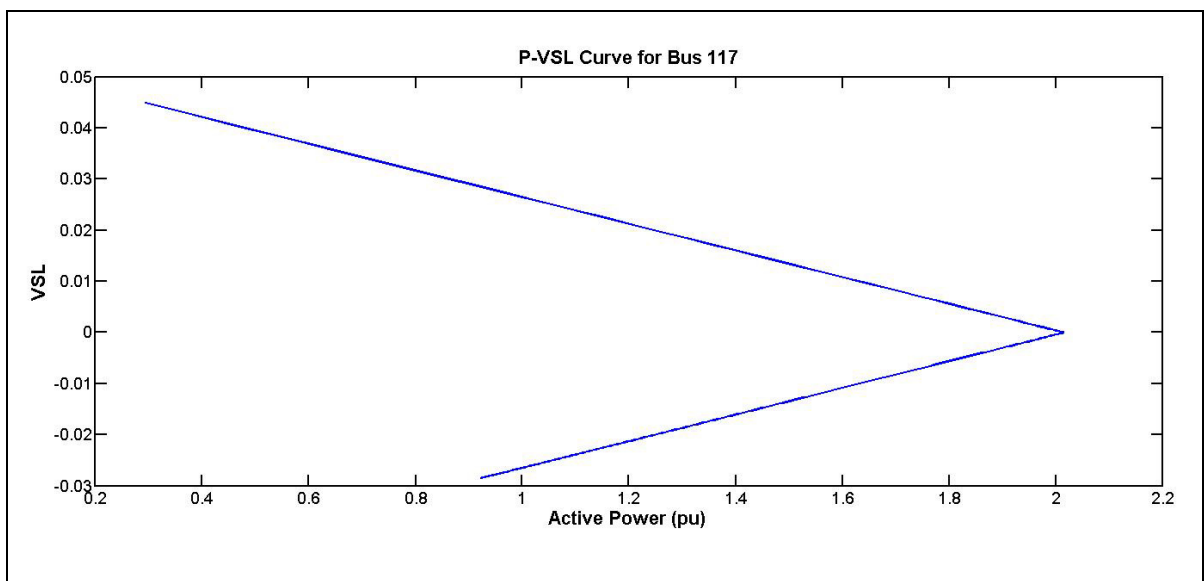


Figure 5.2 P-VSL curve for bus 117

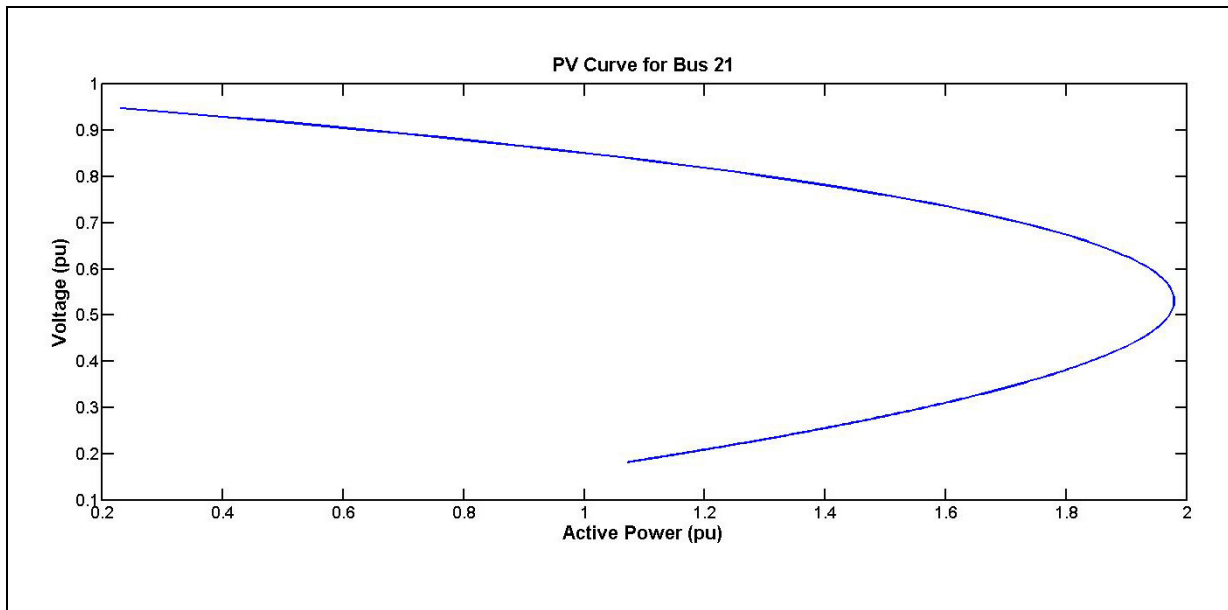


Figure 5.3 PV curve for bus 21

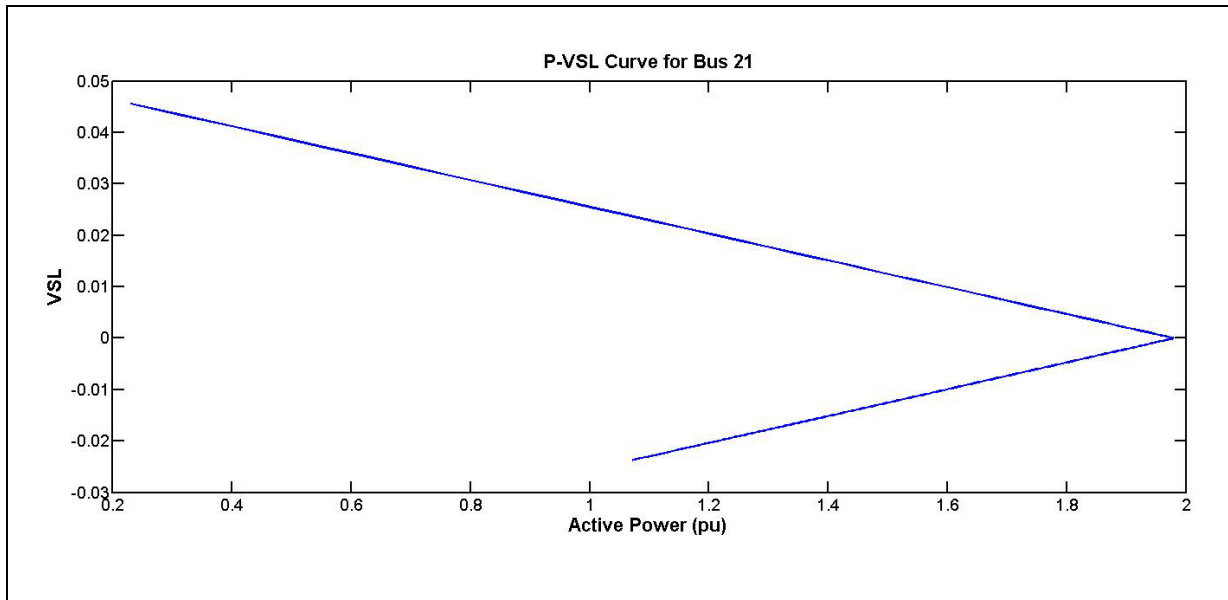


Figure 5.4 P-VSL curve for bus 21

Based on the obtained results from the proposed technique, bus 81 is the second strongest bus of the network. As the load connected to this bus gets heavier, the VSL index of bus 81 gets

smaller and becomes 0 at the nose point of the PV curve. Further increase in the demand, results in decreasing the active power delivered to bus 81 as well as decreasing the value of the VSL index. This situation is illustrated in figures 6.7 and 6.8.

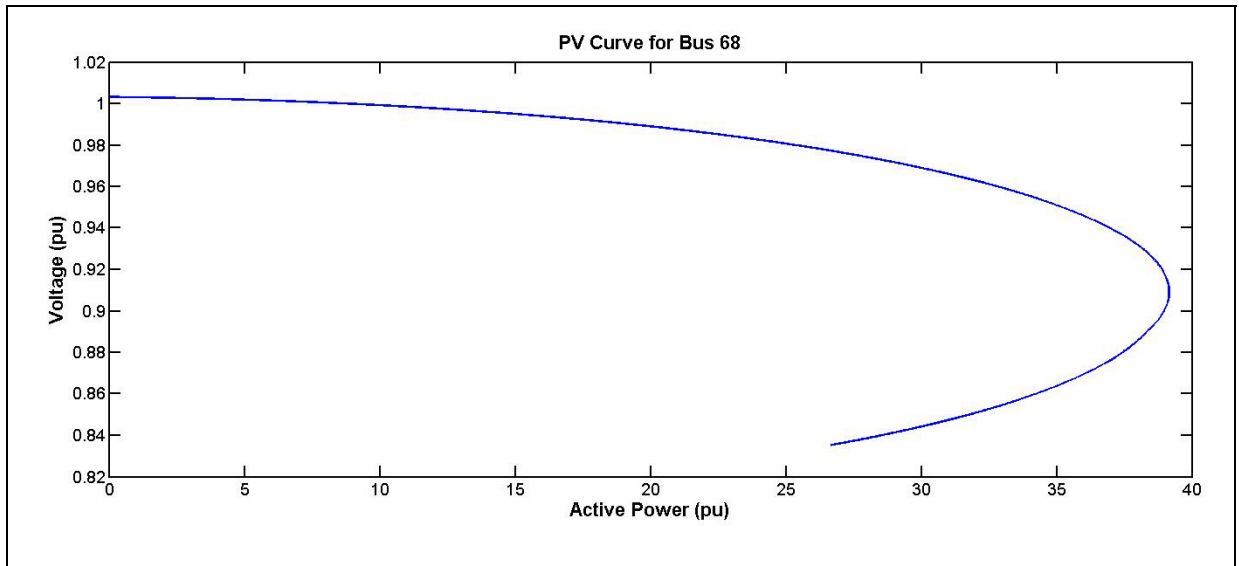


Figure 5.5 PV curve for bus 68

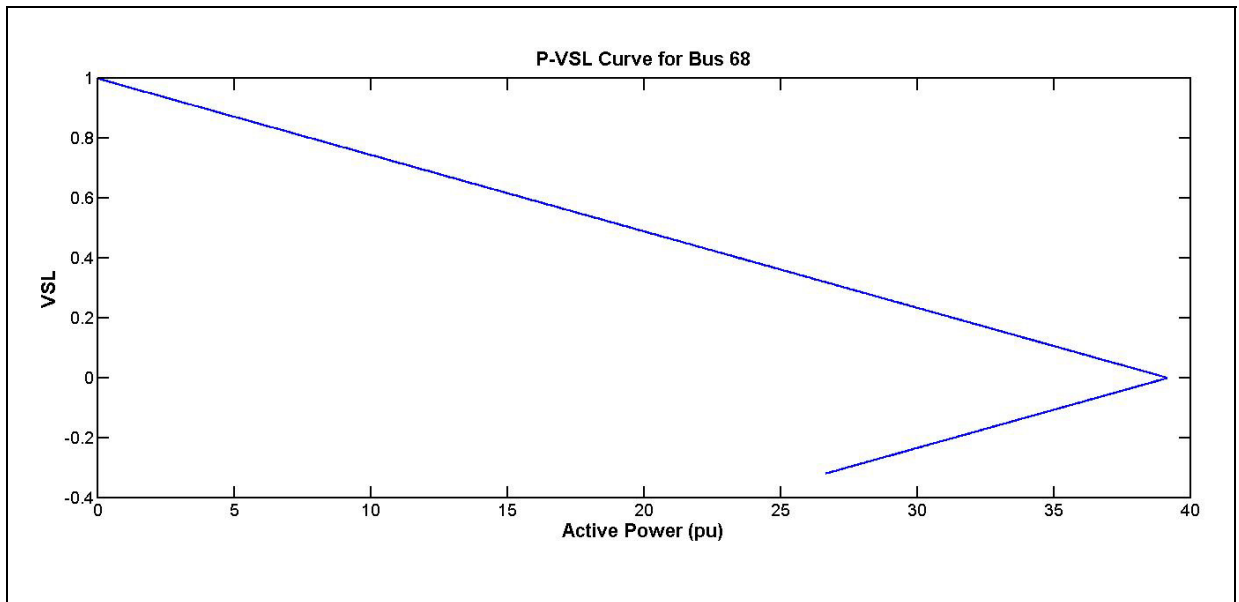


Figure 5.6 P-VSL curve for bus 68

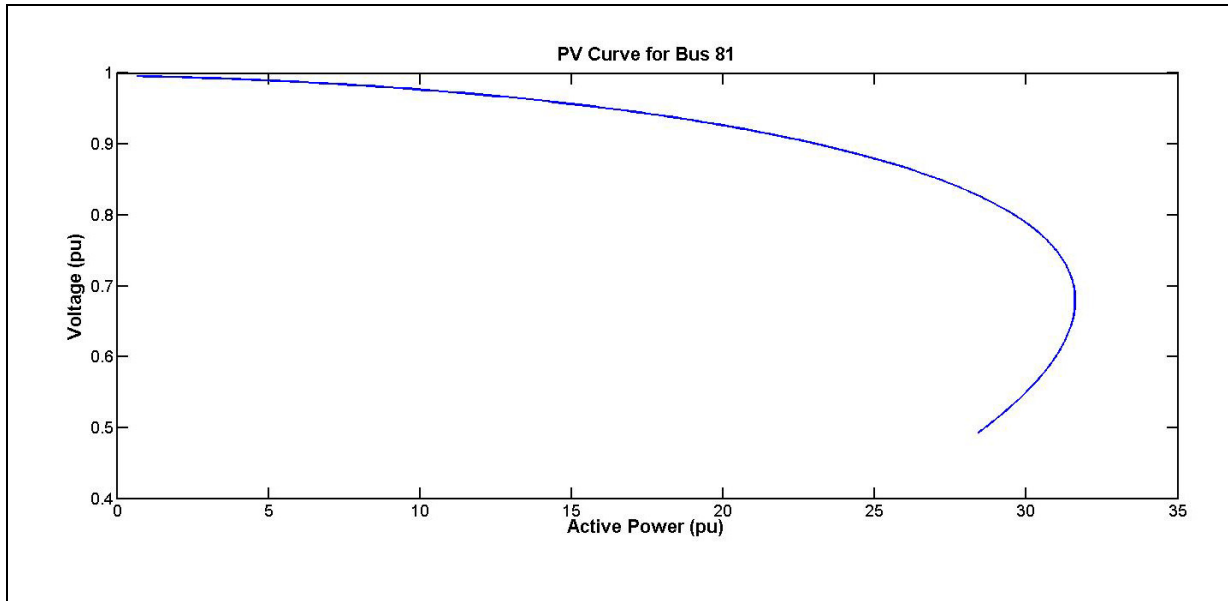


Figure 5.7 PV curve for bus 81

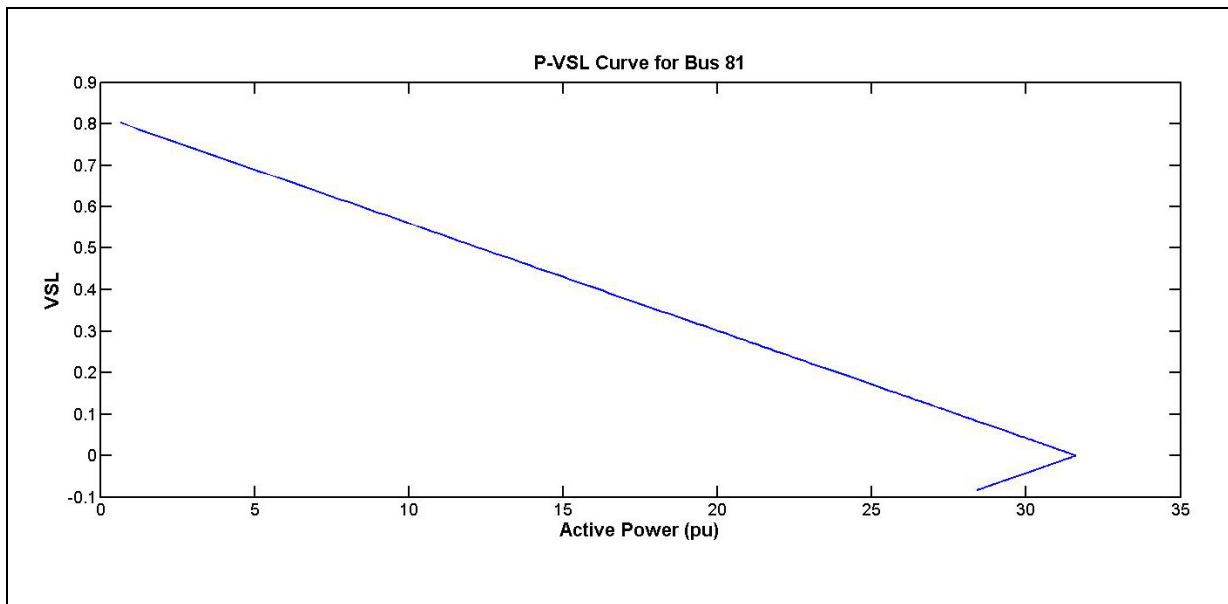


Figure 5.8 P-VSL curve for bus 81

Based on the obtained results from the proposed technique, bus 81 is the second strongest bus of the network. As the bus load gets heavier, the VSL index of bus 81 gets smaller and becomes 0 at the nose point of the PV curve. Further increase in the demand, results in

decreasing the active power delivered to bus 81 as well as decreasing the value of the VSL index. This situation is illustrated in figures 5.7 and 5.8.

5.1.2 Case 2 Hydro-Quebec network

VSL indices were calculated for all the load buses. The three weakest and strongest buses of the Hydro-Quebec network are tabulated in tables 5.3 and 5.4 respectively.

Table 5.3 The three weakest buses of Hydro-Quebec network

Bus number	P_i (pu)	Q_i (pu)	P_{mi} (pu)	Q_{mi} (pu)	VSL
638	0.646	0.148	0.952	0.218	0.011
559	0.056	0.011	0.453	0.0848	0.014
634	0	0	0.389	0	0.014

Table 5.4 The three strongest buses of Hydro-Quebec network

Bus number	P_i (pu)	Q_i (pu)	P_{mi} (pu)	Q_{mi} (pu)	VSL
141	0	0	27.111	0	1
261	0	0	24.315	0	0.934
408	2.84	0.37	24.005	3.336	0.840

Based on the results obtained, bus 638 is the weakest bus and bus 141 is the strongest bus of the network. The active power consumption of the load located at bus 638 is 0.646 pu. According to Table 5.3, if the demand at bus 638 is increased to about 0.96 pu, the Hydro-Quebec system will become unstable because the maximum loadability limit of bus 638 is less than 0.96 pu. The PV and the VSL-Active Power Curves for bus 638 are depicted in

figures 5.9 and 5.10 respectively. The VSL index for this bus at the given load condition is 0.011. This small value for the VSL index implies a very small loadability margin for bus 638.

According to the VSL indices obtained for Hydro-Quebec network, bus 634 is the third weakest bus of the network. This bus reaches its maximum loadability limit at $P=0.389$ pu. Figure 5.11 illustrate the PV curve of bus 634. It can be seen from Figure 5.12 that as the operating point moves on the PV curve toward the nose point, the VSL index of this bus decreases from 0.014 to 0. The VSL index becomes negative when the operating point moves to the lower portion of the PV curve.

Based on the results obtained from the VSL indices, bus 141 is the strongest bus of the Hydro-Quebec network. The maximum loadability limit of this bus is 27.111 pu. The voltage instability phenomenon is likely to initiate from bus 141 because of this large loadability margin of this bus. The PV and VSL-Active Power Curves for bus 638 are depicted in figures 5.13 and 5.14 respectively.

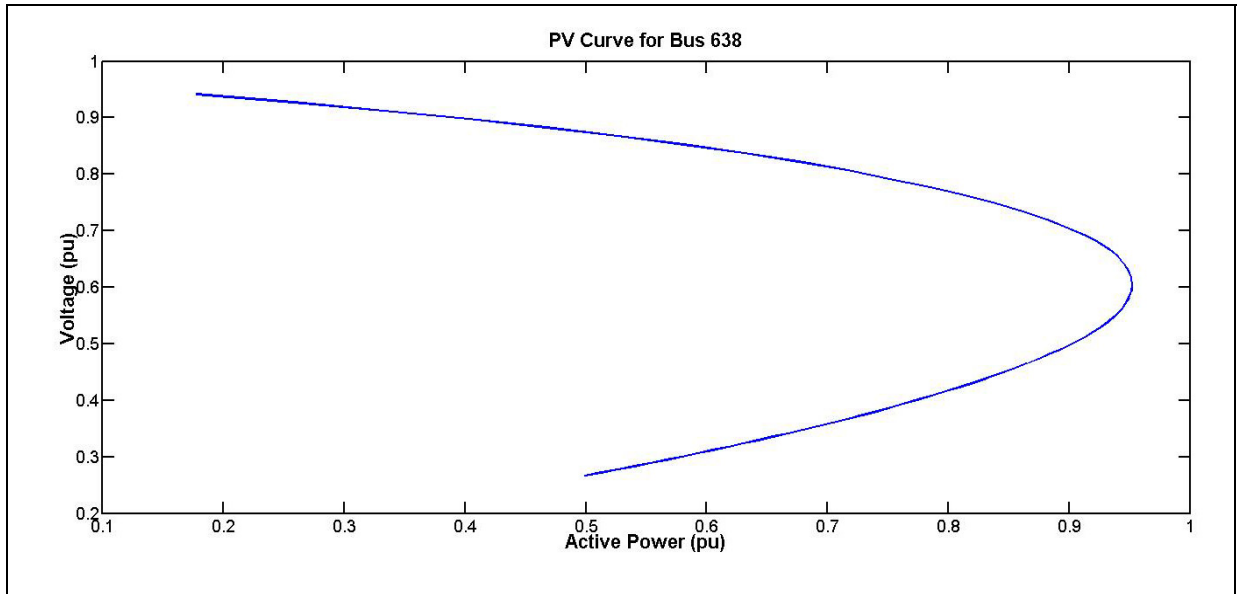


Figure 5.9 PV curve for bus 638

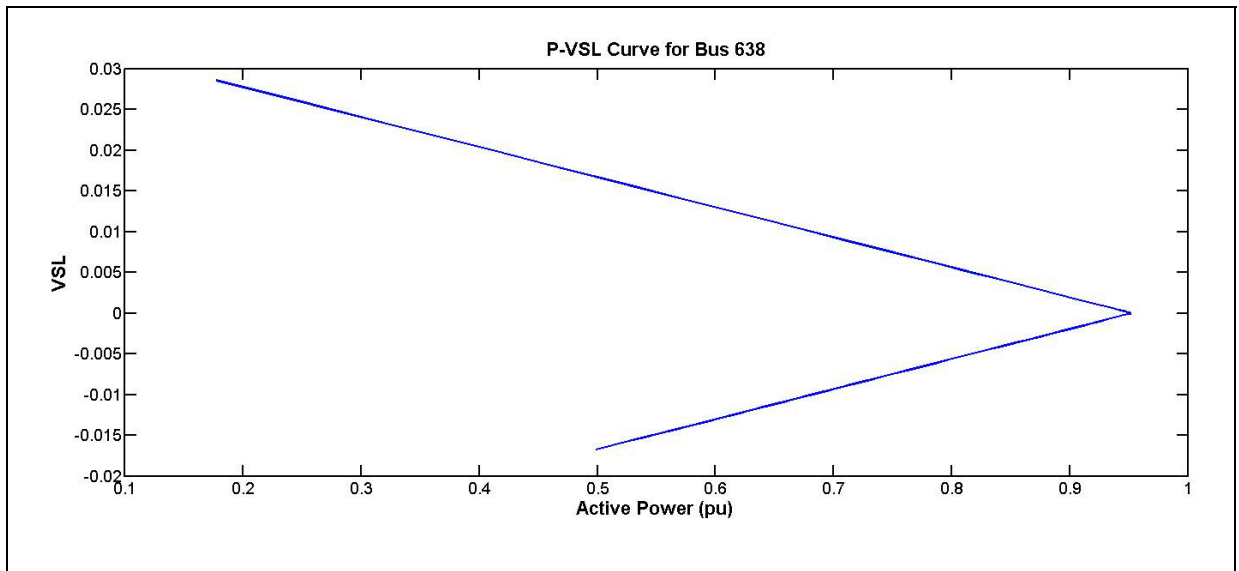


Figure 5.10 P-VSL curve for bus 638

The second strongest bus of the Hydro-Quebec network is bus 261 whose maximum loadability limit is 24.315 pu. The PV and VSL-Active Power Curves for bus 261 are depicted in figures 5.15 and 5.16 respectively.

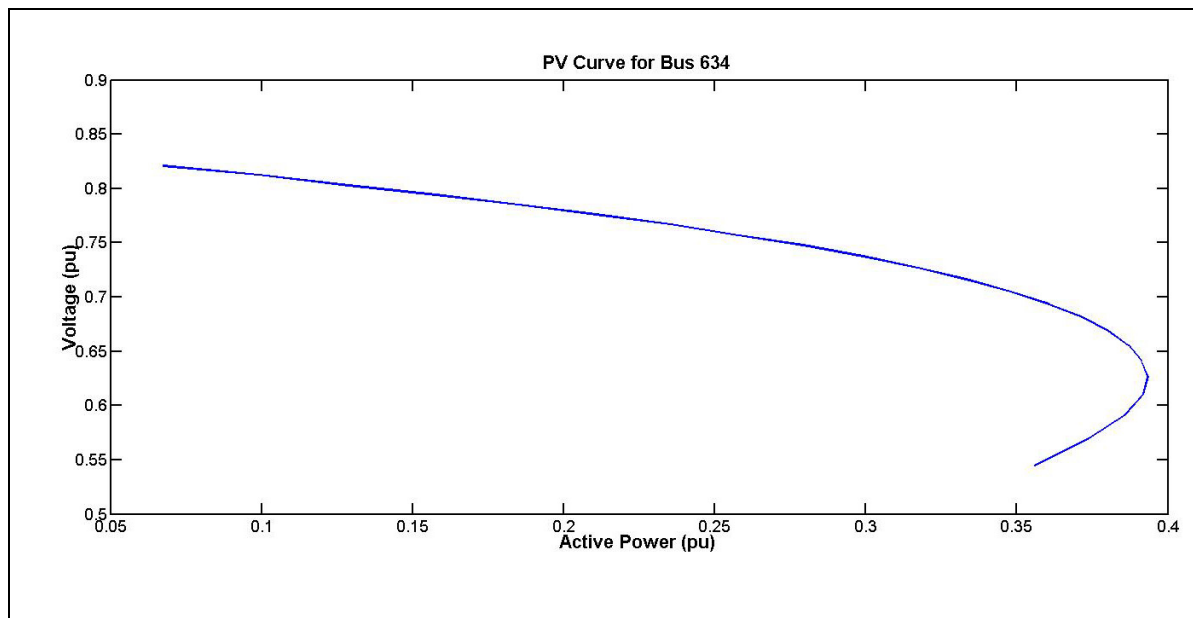


Figure 5.11 PV curve for bus 634

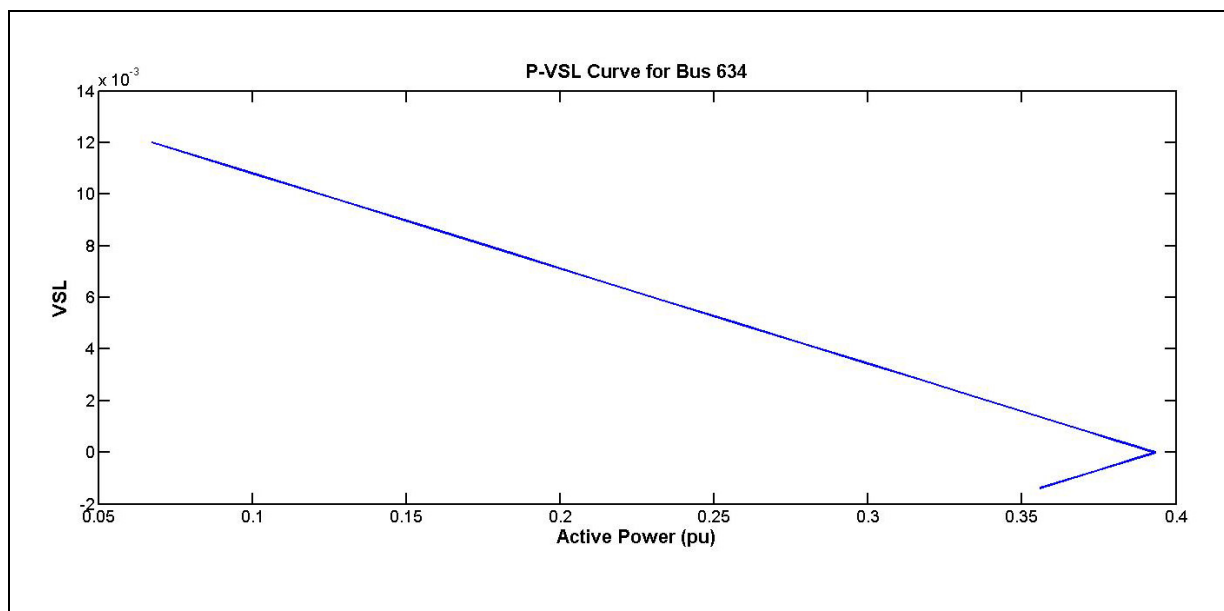


Figure 5.12 P-VSL curve for bus 634

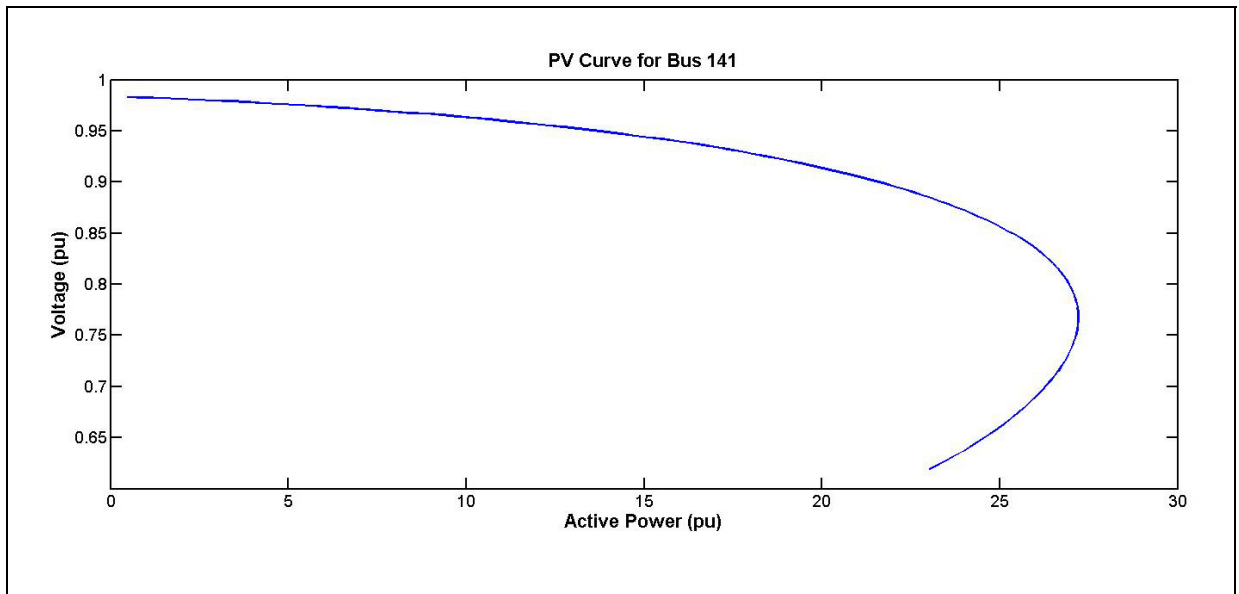


Figure 5.13 PV curve for bus 141

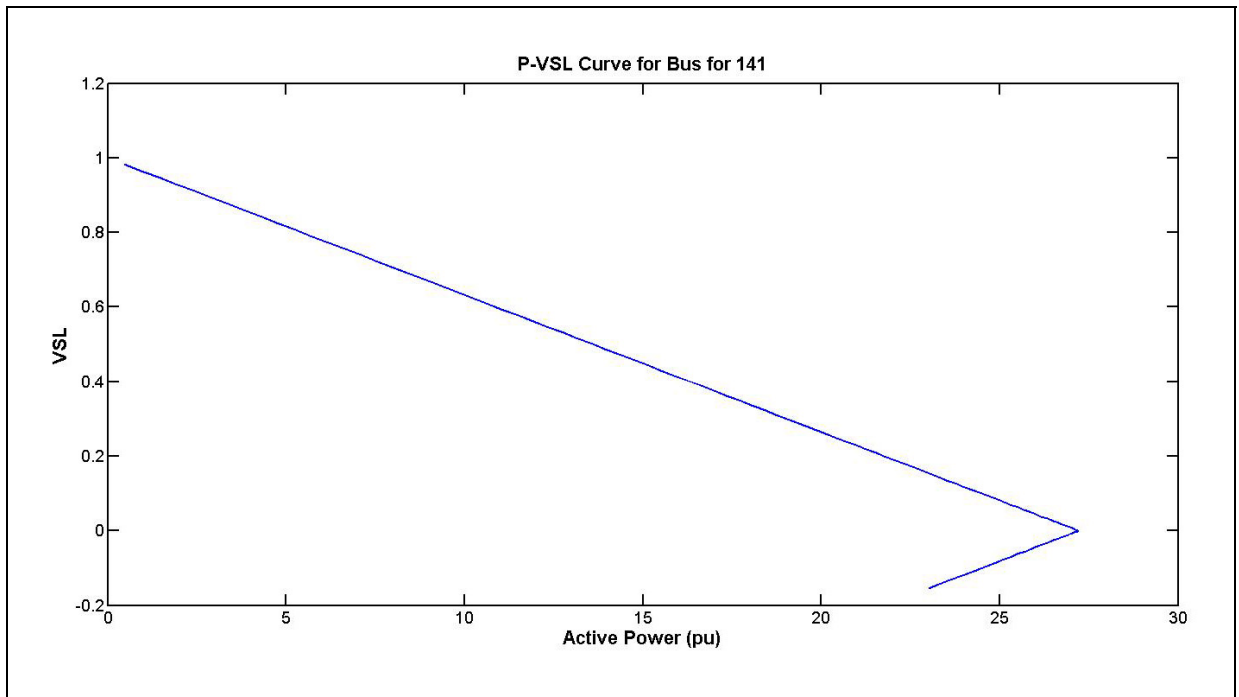


Figure 5.14 P-VSL curve for bus 141

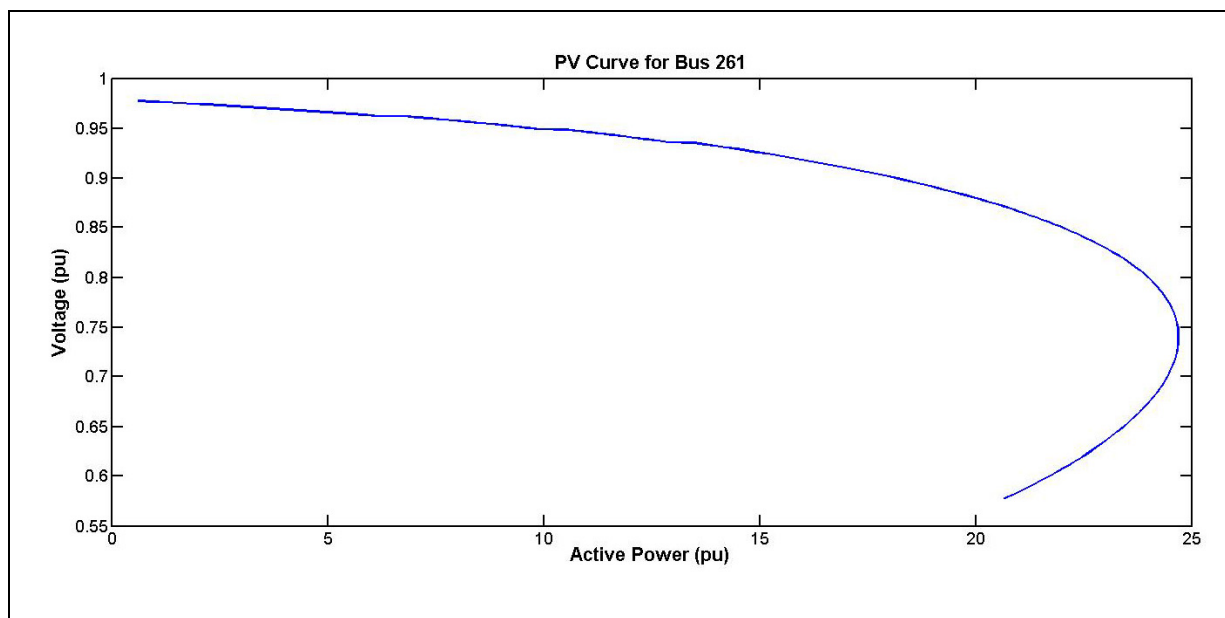


Figure 5.15 PV curve for bus 261

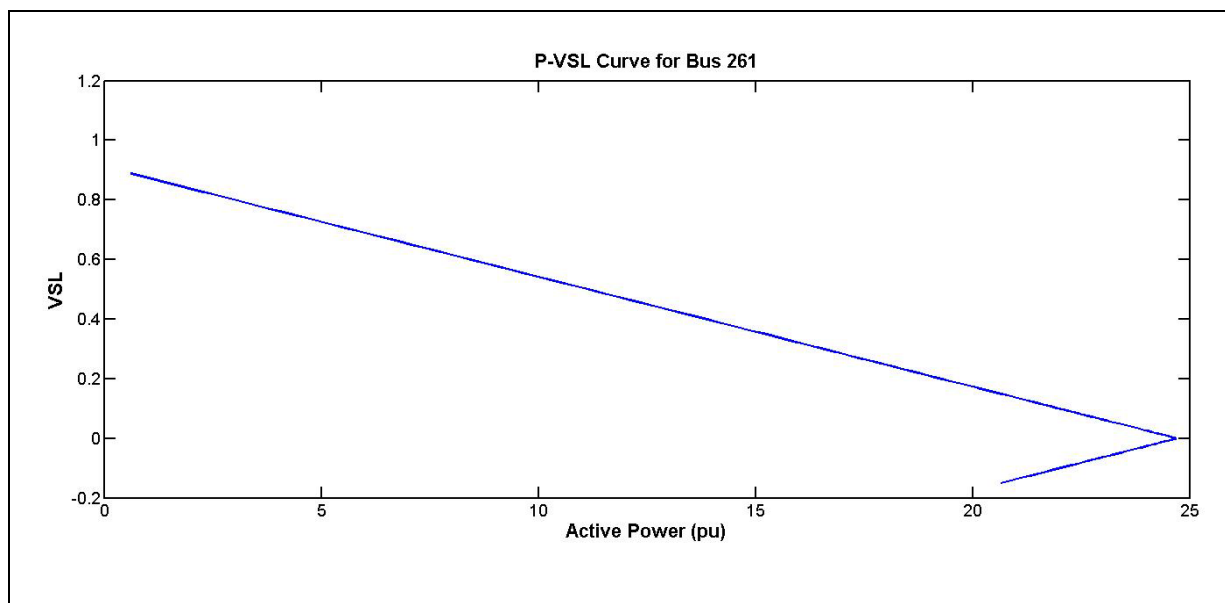


Figure 5.16 P-VSL curve for bus 261

5.1.3 Case 3: 2736-Bus system

The VSL indices were computed for all the load buses. The results for three weakest and three strongest buses of this test case are tabulated in tables 5.5 and 5.6 respectively.

Table 5.5 The three weakest buses of 2736-Bus system

Bus number	P_i (pu)	Q_i (pu)	P_{mi} (pu)	Q_{mi} (pu)	VSL
2164	0.063	0.743	0.191	23.312	0.002
506	0.032	0.010	0.561	0.172	0.006
2166	0.010	0.004	0.761	0.259	0.009

Table 5.6 The three strongest buses of 2736-Bus system

Bus number	P_i (pu)	Q_i (pu)	P_{mi} (pu)	Q_{mi} (pu)	VSL
92	0	0	54.928	0	1
90	0	0	48.892	0	0.890
89	0	0	48.891	0	0.890

Based on the results obtained from VSL index analysis, the weakest bus of this system is bus 2164 which has the maximum loadability of 0.191 pu. Buses 506 and 2166 are the two next weakest buses of 2736-Bus system with the maximum loadabilities of 0.561 pu and 0.761 pu respectively.

Figures 5.17 and 5.18 demonstrate the PV and VSL-Active Power curves for bus 2164. It can clearly be seen that the delivered active power corresponding to the nose point of the PV

curve coincide to the point where the value of the VSL index becomes zero. The same scenario applies to bus 506 which is the second weakest bus of this system (figures 5.19 and 5.20).

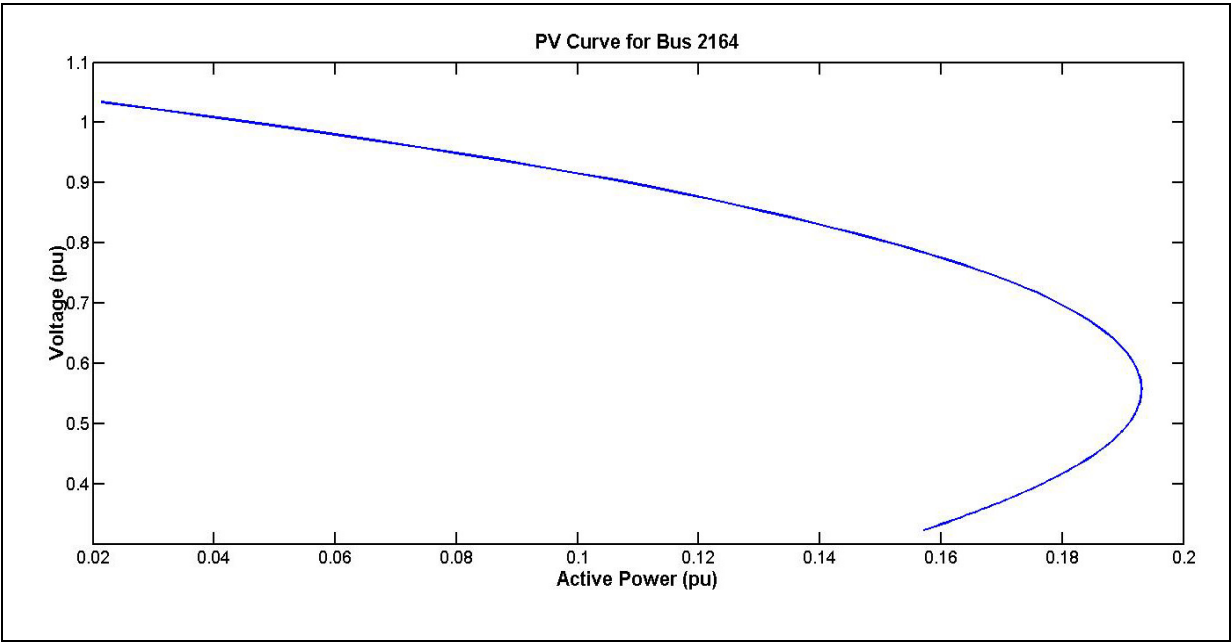


Figure 5.17 PV curve for bus 2164

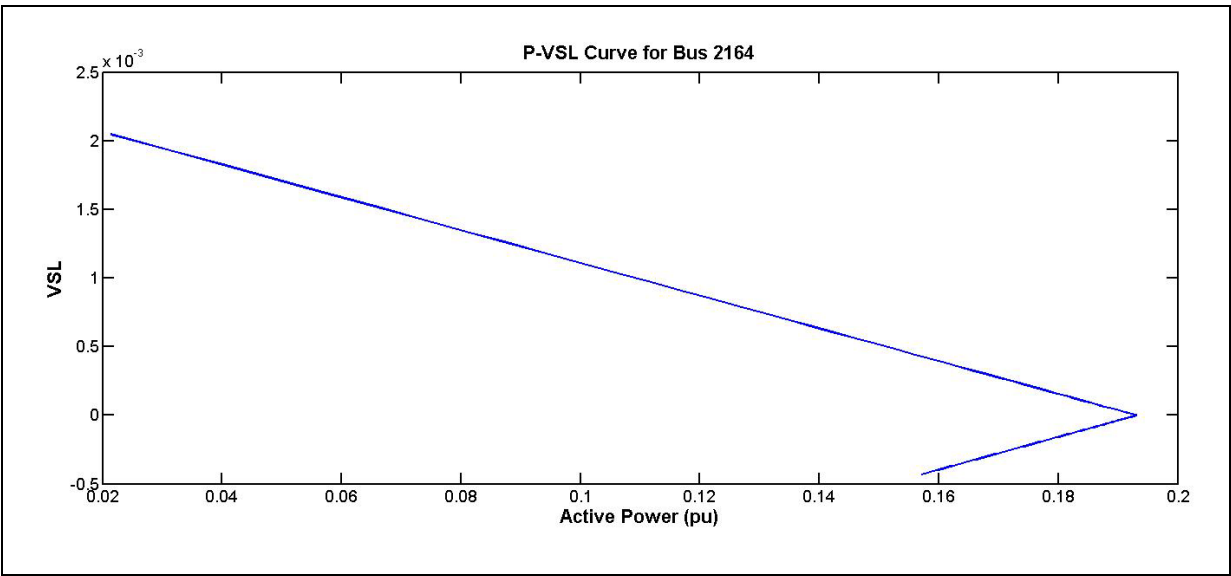


Figure 5.18 P-VSL curve for bus 2164

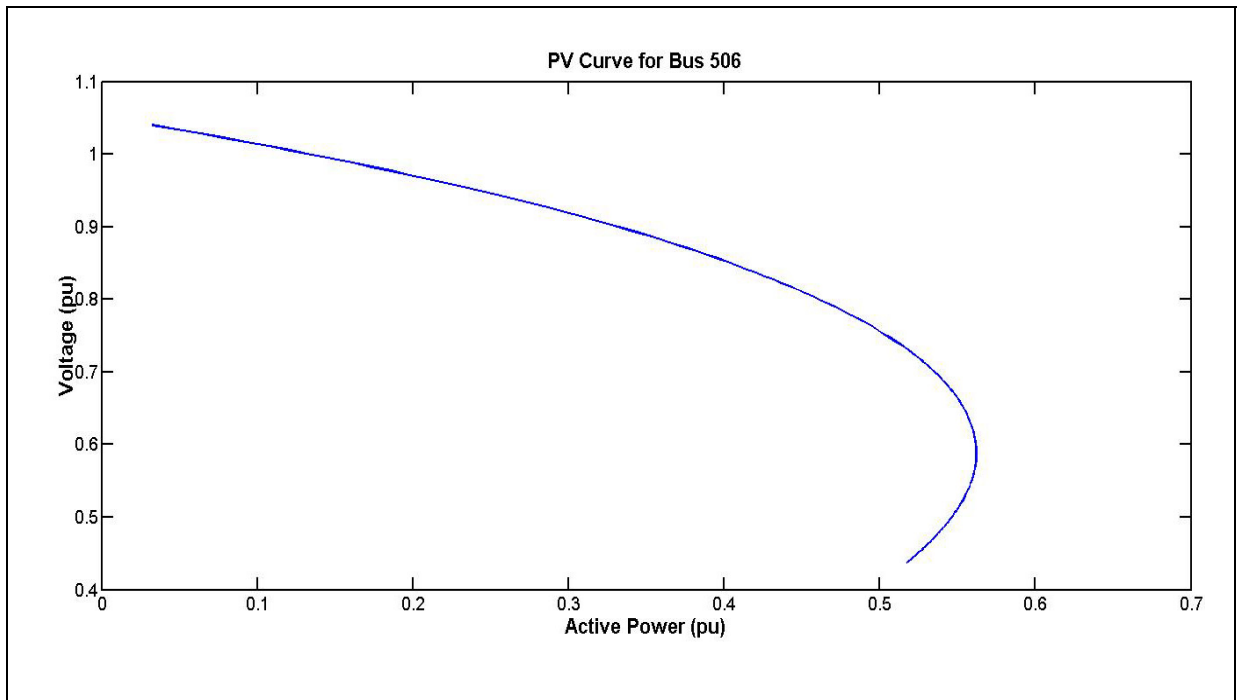


Figure 5.19 PV curve for bus 506

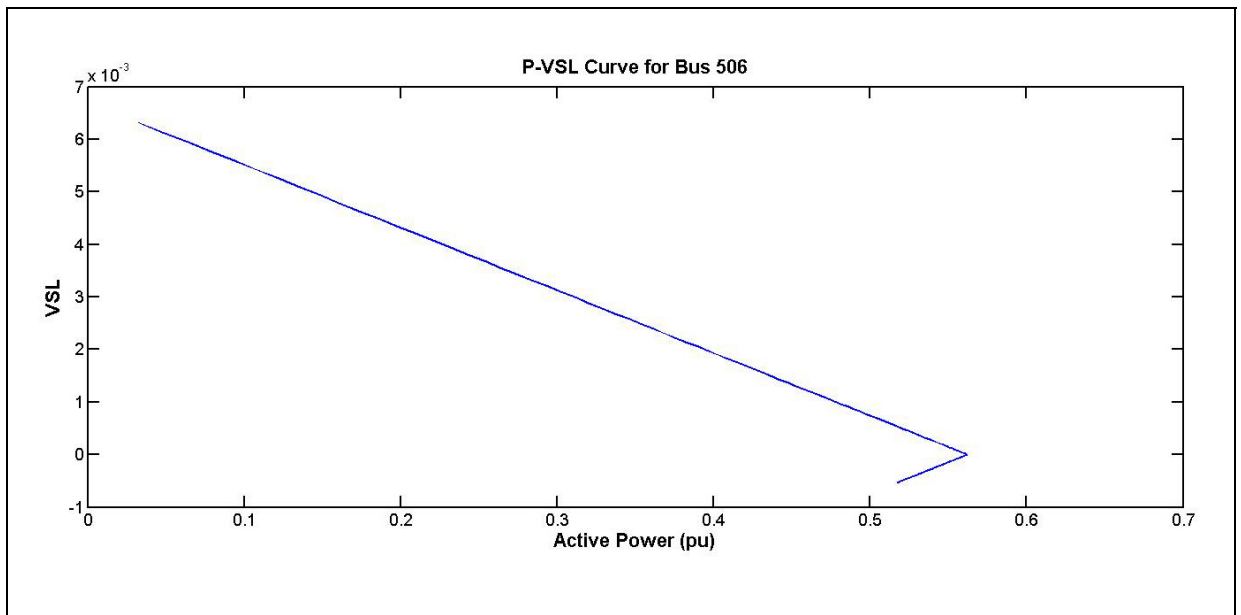


Figure 5.20 P-VSL curve for bus 506

Bus 92 has the largest stability margin and therefore it is considered as the strongest bus of this system. Figures 5.21 and 5.22 demonstrate the PV and VSL-Active Power curves for bus 92.

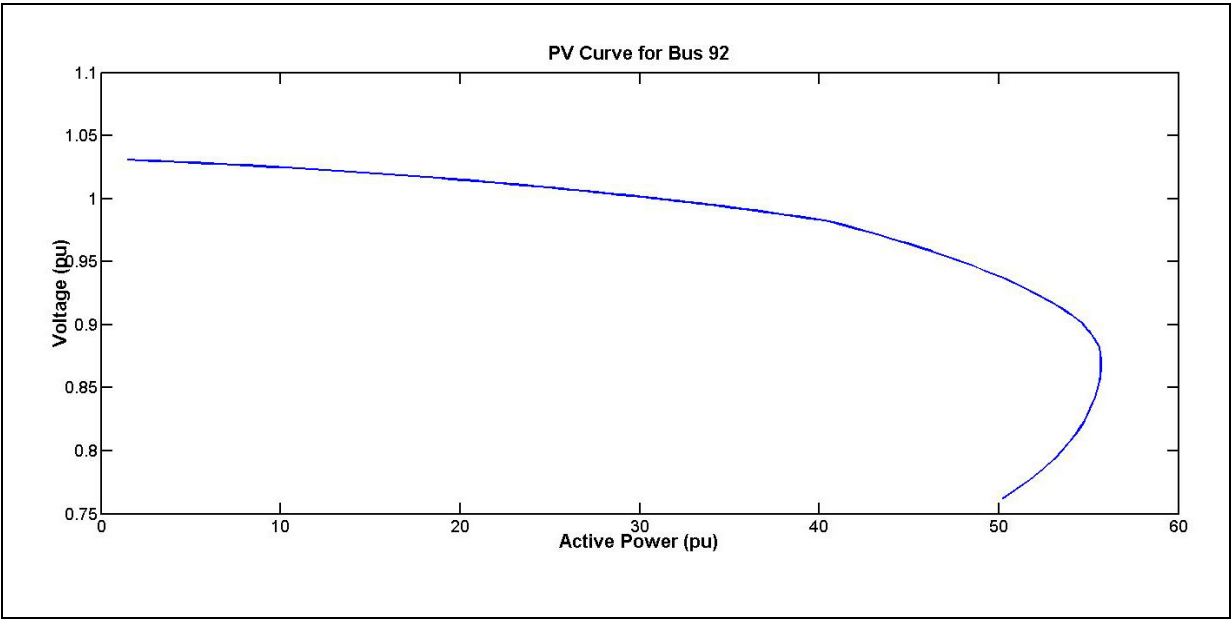


Figure 5.21 PV curve for bus 92

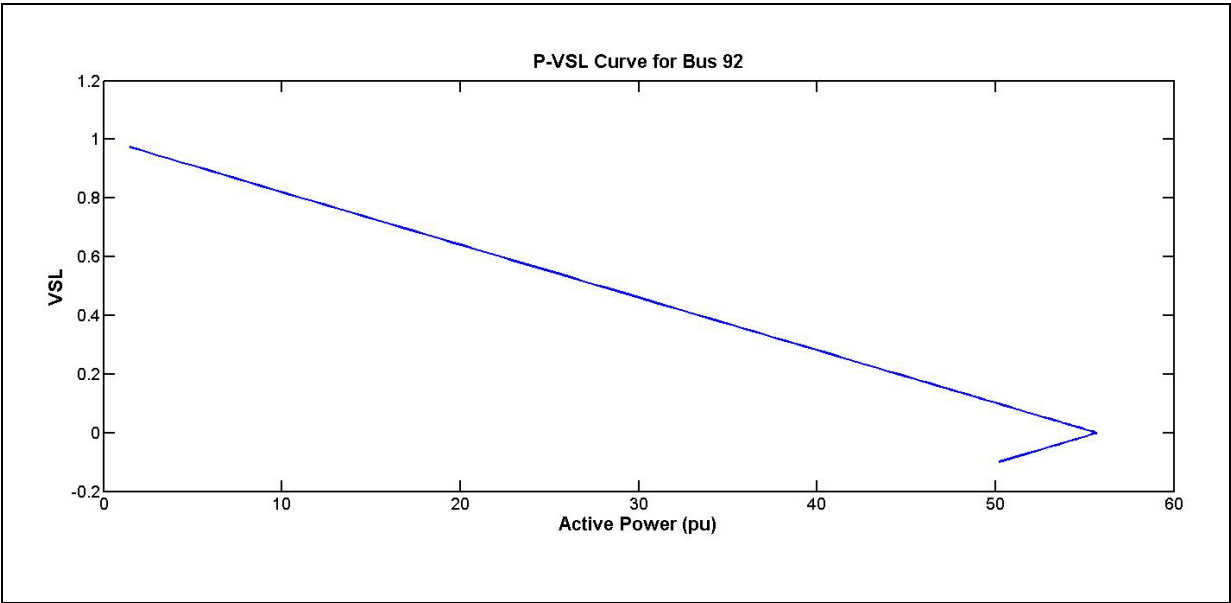


Figure 5.22 P-VSL curve for bus 92

The PV curve characteristic of bus 89 is quite similar to the PV curve characteristic of bus 90 but considering the third decimal point of the maximum loadability limits of these two buses, we chose Bus 90 as the second strongest bus of 2736-Bus system. The PV and VSL-Active Power Curves for bus 90 are depicted in figures 5.23 and 5.24 respectively.

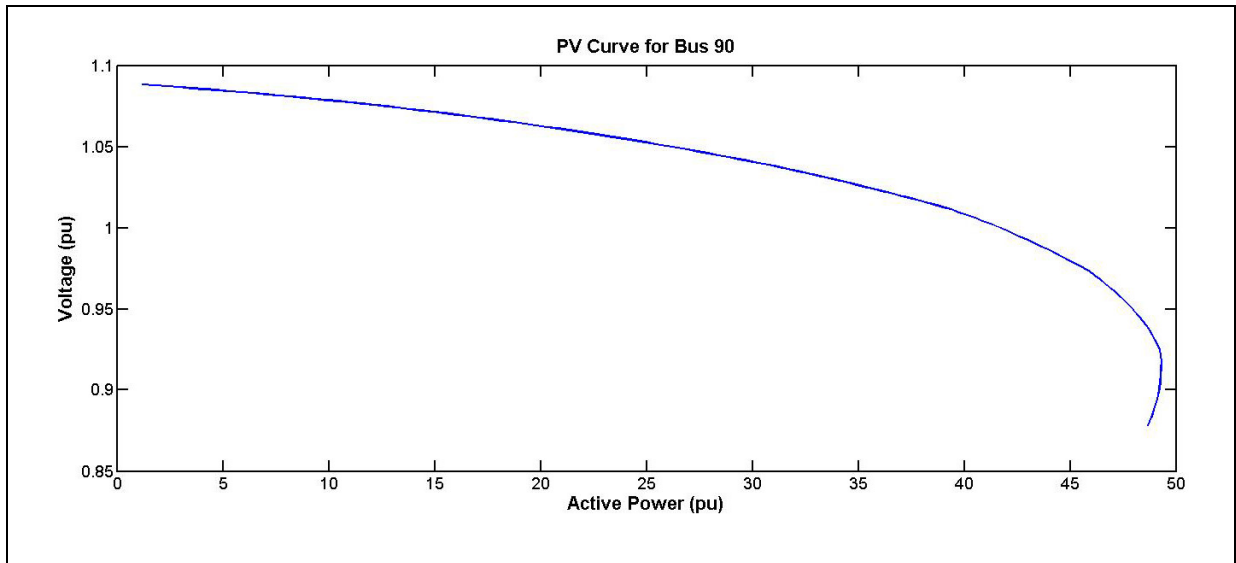


Figure 5.23 PV curve for bus 90

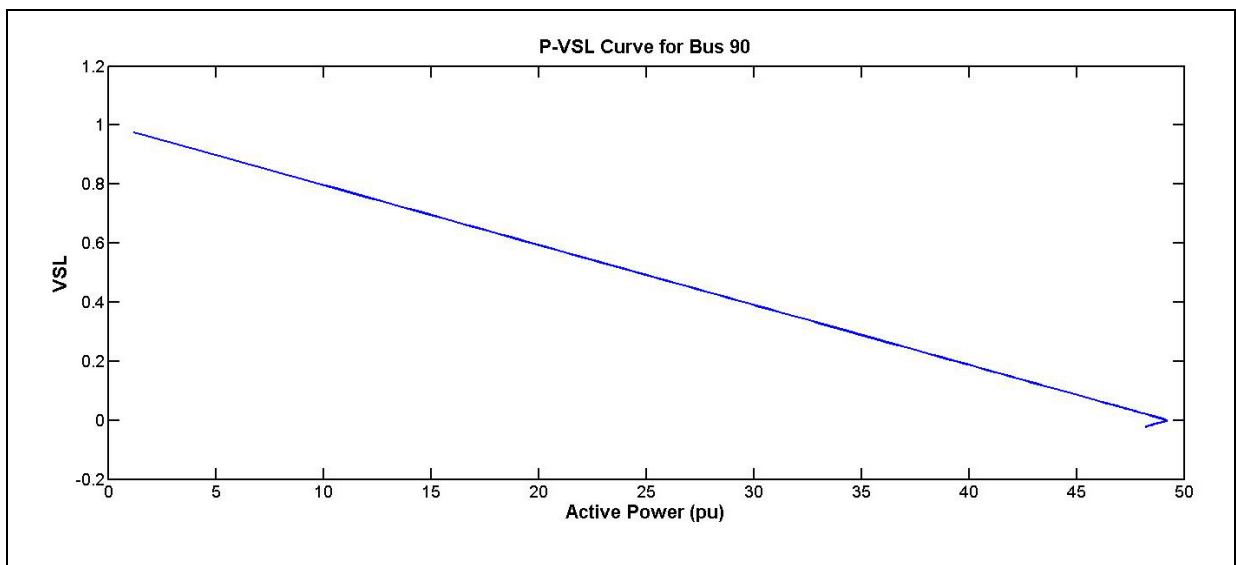


Figure 5.24 P-VSL curve for bus 90

5.2 Comparison to L-index

5.2.1 Case 1: IEEE 118-Bus system

In this section of the thesis, the results obtained from VSL index analysis are compared to the results obtained from L-index which is the most well-known voltage stability index available in the literature.

The PV curves were drawn for all the load buses and the maximum loadability of all the load buses were obtained based on their corresponding PV curves. It is to be noted that to draw the PV curves, power factor of each load was kept constant. The power factors of those load buses which no load has connected to them, were assumed to be unity. Bus 68 has the maximum loadability of 39.472 which is the maximum value among the maximum loadability of all the load buses.

The loadability margin of the weakest buses of the IEEE 118-Bus system based on the L-index and VSL index are tabulated in tables 5.7 and 5.8 respectively. In all the tables of this section, “Loadability margin-1” refers to the loadability calculated using equation 1.17, and “Loadability margin-2” refers to the loadability margin calculated using equation 1.16.

Tables 5.7 and 5.8 clearly demonstrate that the loadability margins obtained from equation 1.16 have nothing to do with the voltage stability. Comparing the loadability margins obtained from equation 1.17, one can conclude that the buses detected by VSL index have the smaller loadability margins than those detected by L-index. Bus 44 is detected by L-index as the weakest bus whereas Table 5.8 demonstrates that there are two buses in this network having smaller loadability margins than bus 44. Although in this section we only compare three weakest and three strongest buses detected by each approach but it is to be noted that according to the VSL index, bus 45 – which according to L-index is the second weakest bus – is the 10th weakest bus (see APPENDIX I).

Table 5.7 Loadability margin of the weakest buses of IEEE 118-Bus system obtained from L-index

Bus number	P_{mi}	Loadability margin-1	Loadability margin-2
44	2.0214	0.0472	0.9208
45	3.8428	0.0839	0.8621
95	4.7528	0.1098	0.9116

Table 5.8 Loadability margin of the strongest buses of IEEE 118-Bus system obtained from VSL- index

Bus number	P_{mi}	Loadability margin-1	Loadability margin-2
117	2.0145	0.0460	0.9007
21	1.9790	0.0466	0.9293
44	2.0214	0.0472	0.9208

The loadability margin of three strongest buses of the IEEE 118-Bus system based on the L-index and VSL index are tabulated in tables 5.9 and 5.10 respectively.

Both L-index and VSL index detect bus 69 as the strongest bus of the system. According to L-index bus 71 is stronger than bus 63 which is not correct because bus the loadability margin of bus 63 is larger than the loadability margin of bus 71. Table 5.10 shows that the loadability margins of both bus 81 and 64 are larger than those obtained for bus 71 and 63. Therefore the results of VSL indices are more accurate than those of L indices.

Table 5.9 Loadability margin of the strongest buses of IEEE 118-Bus system obtained from L- index

Bus number	P_{mi}	Loadability margin-1	Loadability margin-2
68	39.472	1	1
71	12.1087	0.3068	1
63	20.5875	0.5216	1

Table 5.10 Loadability margin of the strongest buses of IEEE 118-Bus system obtained from VSL- index

Bus number	P_{mi}	Loadability margin-1	Loadability margin-2
68	39.472	1	1
81	31.6068	0.8007	1
64	27.7047	0.7019	1

5.2.2 Case 2: Hydro-Quebec network

The PV curves were drawn for all the load buses and the maximum loadability of all the load buses were obtained based on their corresponding PV curves. It is to be noted that to draw the PV curves, power factor of each load was kept constant. The power factors of those load buses which no load has connected to them, were assumed to be unity. Bus 141 has the maximum loadability of 27.2018 which is the maximum value among the maximum loadability of all the load buses.

The loadability margin of the weakest buses of the Hydro-Quebec network based on the L-index and VSL index are tabulated in tables 5.11 and 5.12 respectively.

Table 5.11 Loadability margin of the weakest buses of Hydro-Quebec network obtained from L-index

Bus number	P_{mi}	Loadability margin-1	Loadability margin-2
638	0.9516	0.0112	0.3215
634	0.3933	0.0145	1
678	1.9749	0.1098	0.9116

Table 5.12 Loadability margin of the weakest buses of Hydro-Quebec network obtained from VSL- index

Bus number	P_{mi}	Loadability margin-1	Loadability margin-2
638	0.9516	0.0112	0.3215
559	0.4596	0.0102	0.8784
634	0.3933	0.0145	1

Bus 638 was detected by both L-index and VSL index as the weakest bus of Hydro-Quebec network. According to the L-index bus 634 is the second weakest bus whereas according to the VSL index bus 634 is the third weakest bus. Figure 5.12 illustrates that the weakest bus of this power system is bus 559 whose loadability margin is 0.0102. The error of VSL index is only 0.001 but even this slight error has caused replacing the weakest bus of the network by the second weakest bus of the network. The occurred error is because to compute the VSL index of each bus, the maximum loadabilities obtained by the P & O algorithm proposed in Chapter 4 have been used. According to the result obtained by P & O algorithm the maximum loadability of bus 559 is 0.4313 whereas the actual maximum loadability of this bus is 0.4596.

The loadability margin of three strongest buses of Hydro-Quebec network based on the L-index and VSL index are tabulated in tables 5.13 and 5.14 respectively.

Table 5.13 Loadability margin of the strongest buses of Hydro-Quebec network obtained from L- index

Bus number	P_{mi}	Loadability margin-1	Loadability margin-2
64	4.9982	0.1837	1
65	5.4979	0.2021	1
146	20.2203	0.7433	1

Table 5.14 Loadability margin of the strongest buses of Hydro-Quebec network obtained from VSL- index

Bus number	P_{mi}	Loadability margin-1	Loadability margin-2
141	27.2018	1	1
261	24.6942	0.9078	1
408	24.3587	0.7911	0.8834

According to L-index bus 64 is the strongest bus of the system whereas according to VSL index this bus is considered to be a weak bus. Comparing the loadability margins of the buses detected by L-index and VSL index, it can be clearly concluded that the VSL index provides more accurate results.

5.2.3 Case 3: 2736-Bus system

To find the bus which has the maximum loadability limit in 2736-Bus system, PV curves were drawn for 50 buses having largest VSL indices. Considering the results of VSL indices for IEEE 18-Bus system and Hydro-Quebec network it is very less likely that the P & O algorithm proposed in chapter 4 has missed the bus which has the largest loadability limit. Bus 92 has the maximum loadability limit of 55.6561 which is the largest loadability limit among all the load buses of this system.

The loadability margin of the weakest buses of 2736-Bus system based on the L-index and VSL index are tabulated in tables 5.15 and 5.16 respectively. Maximum loadability of each bus (P_{mi}) was obtained from its PV curve.

Bus 506 appears as one of the three weakest buses of this power system, from the results obtained by both L-index and VSL index techniques. Although buses 260 and 250 have very small loadability margins indicating the weakness of these buses but there are some buses in this network whose loadability margins are smaller than these two buses. Therefore buses 260 and 250 are not the second and third weakest buses of 2736-Bus system. Two of the buses which are weaker than buses 260 and 250 are shown in Table 5.16.

Table 5.15 Loadability margin of the weakest buses of 2736-Bus system obtained from L-index

Bus number	P_{mi}	Loadability margin-1	Loadability margin-2
506	0.5615	0.0095	0.9431
260	0.9441	0.0161	0.9492
250	1.011	0.0175	0.7365

Table 5.16 Loadability margin of the weakest buses of 2736-Bus system obtained from VSL index

Bus number	P_{mi}	Loadability margin-1	Loadability margin-2
2164	0.1923	0.0023	0.6708
506	0.5615	0.0095	0.9431
2166	0.7721	0.0137	0.9866

The loadability margin of three strongest buses of 2736-Bus system based on the L-index and VSL index are tabulated in tables 5.17 and 5.18 respectively.

Comparing the loadability margins of the buses recognized by L-index to the loadability margins of the buses recognized by VSL index (tables 5.17 and 5.18), one can conclude that L-index totally fails to detect the strong buses of this power system. All the three buses detected by L-index as the three strongest buses of this system, have relatively small loadability margins.

Table 5.17 Loadability margin of the strongest buses of
2736-Bus system obtained from L- index

Bus number	P_{mi}	Loadability margin-1	Loadability margin-2
1963	3.645	0.0655	1
1992	7.6408	0.1373	1
1998	4.1550	0.0747	1

Table 5.18 Loadability margin of the strongest buses of
2736-Bus system obtained from L- index

Bus number	P_{mi}	Loadability margin-1	Loadability margin-2
92	55.6561	1	1
90	49.2176	0.8843	1
89	49.2021	0.8840	1

CONCLUSION

A novel technique to obtain the maximum loadability limits of all the load buses of a power system based on P & O algorithm was proposed in this thesis. Then, a simple method based on the sensitivity of voltage magnitude to the injection of reactive power was suggested to examine the voltage controllability of each bus – i.e whether or not the voltage control equipment has a positive corrective effect. The loadability limits obtained using the P & O algorithm were then employed to calculate the loadability margins of all the load buses. The calculated loadability margins and the suggested method to reveal the voltage controllability condition of every bus were utilized to define a novel voltage stability index named the VSL index. The VSL index is computed for all the load buses and its value lies between -1 and 1. To verify the accuracy and robustness of the proposed index, the IEEE 118-Bus system, Hydro-Quebec network, and 2736-Bus system were taken as case studies. The maximum loadability limits obtained from the proposed algorithm were compared to those of obtained from PV curves and the results confirmed the robustness of the proposed algorithm to estimate the maximum loadability limits in a much shorter time than plotting PV curves for all the load buses. It was shown that a bus which has the largest VSL index is the strongest bus of the power system and conversely, a bus which has the smallest VSL index is the weakest bus of the network. It was also demonstrated that the VSL index is more accurate and reliable than the L-index. In addition to accuracy and reliability, the VSL index together with the maximum loadability limits obtained from the P & O algorithm, provides an absolute measure rather than a relative measure of proximity to voltage instability. This property enables the power system operators to take the required remedial actions to prevent voltage instability from occurring.

RECOMMENDATIONS

- Knowing the loadability limits of the weak buses, the corresponding Thevenin impedance can be computed. Decreasing the magnitude of Thevenin impedance seen from the weak buses, results in increasing their loadability limits. Further research must be carried out to figure out how to decrease the magnitude of the Thevenin impedance seen from each bus;
- A fuzzy based voltage control technique can be developed. The VSL indices of the load buses can form a vector. The objective of the fuzzy-based voltage controller should be to maximize the VSL vector. A sensitivity matrix can be defined to relate the VSL vector to the variations in the reactive power control variables. This sensitivity matrix can provide useful information such as which reactive power source has the most significant effect on the VSL index of a particular bus. The challenge will be how to define appropriate membership functions to optimize the performance of such a fuzzy controller.

APPENDIX I

RESULTS FOR IEEE 118-BUS SYSTEM AND HYDRO-QUEBEC NETWORK

Table-A I-1 VSL indices for IEEE 118-Bus system

Bus number	Pi	Qi	Pmi	Qmi	VSL index
21	0.140	0.080	1.782	1.018	0.043
117	0.200	0.080	2.001	0.800	0.047
44	0.160	0.080	2.039	1.019	0.049
22	0.100	0.050	2.191	1.096	0.054
43	0.180	0.070	2.275	0.885	0.054
53	0.230	0.110	2.812	1.345	0.067
101	0.220	0.150	2.893	1.972	0.069
52	0.180	0.050	2.941	0.817	0.072
45	0.530	0.220	3.831	1.590	0.086
20	0.180	0.030	3.511	0.585	0.086
86	0.000	0.000	3.512	0.000	0.091
13	0.340	0.160	3.902	1.836	0.092
51	0.170	0.080	3.741	1.760	0.093
33	0.230	0.090	3.866	1.513	0.094
58	0.120	0.030	3.763	0.941	0.094
84	0.110	0.070	4.071	2.591	0.103
57	0.120	0.030	4.159	1.040	0.105
95	0.420	0.310	4.728	3.489	0.112
16	0.250	0.100	4.715	1.886	0.116
93	0.120	0.070	4.649	2.712	0.117
98	0.340	0.080	4.952	1.165	0.120
97	0.150	0.090	4.806	2.884	0.121
28	0.170	0.070	5.142	2.117	0.129
108	0.020	0.010	5.129	2.565	0.132
50	0.170	0.040	5.285	1.243	0.133
109	0.080	0.030	5.328	1.998	0.136

Table-A I-1 VSL indices for IEEE 118-Bus system (Cont'd)

Bus number	Pi	Qi	Pmi	Qmi	VSL index
102	0.050	0.030	5.306	3.184	0.136
83	0.200	0.100	5.461	2.730	0.136
39	0.270	0.110	5.759	2.346	0.142
48	0.200	0.110	6.159	3.387	0.154
67	0.280	0.070	6.245	1.561	0.155
106	0.430	0.160	6.614	2.461	0.160
2	0.200	0.090	6.463	2.908	0.162
14	0.140	0.010	6.446	0.460	0.163
118	0.330	0.150	6.810	3.096	0.168
82	0.540	0.270	7.291	3.646	0.175
88	0.480	0.100	7.509	1.564	0.182
41	0.370	0.100	7.509	2.029	0.185
114	0.080	0.030	7.601	2.850	0.195
115	0.220	0.070	7.858	2.500	0.198
3	0.390	0.100	8.317	2.132	0.205
29	0.240	0.040	8.339	1.390	0.210
96	0.380	0.150	8.740	3.450	0.217
79	0.390	0.320	8.851	7.262	0.219
94	0.300	0.160	8.815	4.701	0.221
47	0.340	0.000	9.087	0.000	0.227
38	0.000	0.000	8.829	0.000	0.229
5	0.000	0.000	9.294	0.000	0.241
7	0.190	0.020	9.667	1.018	0.246
11	0.700	0.230	10.322	3.391	0.249
35	0.330	0.090	10.341	2.820	0.260
75	0.470	0.110	10.532	2.465	0.261
9	0.000	0.000	10.637	0.000	0.276

Table-A I-1 VSL indices for IEEE 118-Bus system (Cont'd)

Bus number	Pi	Qi	Pmi	Qmi	VSL index
23	0.070	0.030	10.895	4.669	0.281
17	0.110	0.030	10.976	2.994	0.282
37	0.000	0.000	10.954	0.000	0.284
30	0.000	0.000	11.267	0.000	0.292
71	0.000	0.000	11.611	0.000	0.301
63	0.000	0.000	20.446	0.000	0.530
78	0.710	0.260	21.427	7.847	0.537
60	0.780	0.030	25.674	0.987	0.645
64	0.000	0.000	27.430	0.000	0.711
81	0.000	0.000	31.802	0.000	0.824
68	0.000	0.000	38.577	0.000	1.000

Table-A I-2 VSL indices for Hydro-Quebec network

Bus number	Pi	Qi	Pmi	Qmi	VSL index
638	1	0	0.952	0.218	0.011
559	0	0	0.431	0.085	0.014
634	0	0	0.389	0.000	0.014
640	1	0	1.402	0.374	0.016
436	0	0	0.517	0.207	0.017
451	0	0	0.519	0.111	0.018
695	0	0	0.539	0.137	0.018
452	0	0	0.488	0.000	0.018
455	0	0	0.649	0.160	0.018
649	0	0	0.863	0.256	0.023
454	0	0	0.816	0.203	0.024
641	0	0	0.927	0.278	0.024
678	1	0	1.661	0.432	0.024
694	0	0	0.774	0.155	0.027
450	0	0	0.819	0.190	0.028
462	0	0	0.940	0.284	0.030
553	0	0	1.042	0.329	0.031
433	0	0	0.925	0.211	0.032
424	2	0	2.636	0.273	0.033
555	0	0	1.112	0.066	0.036
557	0	0	1.024	0.000	0.038
522	0	0	1.294	0.178	0.040
412	0	0	1.425	0.296	0.040
525	0	0	1.391	0.341	0.040
453	0	0	1.108	0.000	0.041
446	0	0	1.314	0.232	0.043
447	0	0	1.276	0.205	0.044
563	0	0	1.260	0.420	0.044
328	0	0	1.211	0.000	0.045

Table-A I-2 VSL indices for Hydro-Quebec network (Cont'd)

Bus number	Pi	Qi	Pmi	Qmi	VSL index
577	0	0	1.329	0.362	0.045
432	1	0	1.979	0.403	0.047
526	0	0	1.276	0.000	0.047
445	0	0	1.301	0.000	0.048
628	0	0	1.624	0.541	0.049
461	0	0	1.377	0.000	0.051
434	0	0	1.606	0.401	0.055
431	0	0	1.601	0.364	0.058
483	0	0	1.692	0.278	0.058
487	0	0	1.975	1.129	0.059
572	0	0	1.731	0.519	0.060
444	1	0	2.974	0.654	0.061
430	0	0	1.657	0.000	0.061
545	1	0	2.332	0.123	0.062
767	2	1	3.699	2.035	0.062
414	0	0	1.701	0.000	0.063
556	0	0	1.705	0.000	0.063
429	0	0	1.761	0.328	0.064
334	0	0	1.843	0.298	0.065
637	0	0	1.764	0.000	0.065
439	0	0	2.282	0.617	0.068
441	0	0	2.098	0.606	0.068
438	0	0	2.018	0.605	0.069
648	0	0	1.904	0.000	0.070
443	0	0	2.160	0.510	0.070
428	0	0	1.938	0.000	0.071
435	0	0	1.974	0.000	0.073

Table-A I-2 VSL indices for Hydro-Quebec network (Cont'd)

Bus number	Pi	Qi	Pmi	Qmi	VSL index
526	0	0	1.276	0.000	0.047
445	0	0	1.301	0.000	0.048
628	0	0	1.624	0.541	0.049
461	0	0	1.377	0.000	0.051
434	0	0	1.606	0.401	0.055
431	0	0	1.601	0.364	0.058
483	0	0	1.692	0.278	0.058
487	0	0	1.975	1.129	0.059
572	0	0	1.731	0.519	0.060
444	1	0	2.974	0.654	0.061
430	0	0	1.657	0.000	0.061
545	1	0	2.332	0.123	0.062
767	2	1	3.699	2.035	0.062
414	0	0	1.701	0.000	0.063
556	0	0	1.705	0.000	0.063
429	0	0	1.761	0.328	0.064
334	0	0	1.843	0.298	0.065
637	0	0	1.764	0.000	0.065
439	0	0	2.282	0.617	0.068
441	0	0	2.098	0.606	0.068
438	0	0	2.018	0.605	0.069
648	0	0	1.904	0.000	0.070
443	0	0	2.160	0.510	0.070
428	0	0	1.938	0.000	0.071
435	0	0	1.974	0.000	0.073

Table-A I-2 VSL indices for Hydro-Quebec network (Cont'd)

Bus number	Pi	Qi	Pmi	Qmi	VSL index
268	0	0	2.066	0.516	0.073
564	1	0	2.686	0.365	0.074
437	0	0	2.090	0.000	0.077
440	0	0	2.094	0.000	0.077
576	1	0	2.821	0.398	0.078
625	0	0	2.106	0.000	0.078
654	1	0	2.634	0.287	0.078
442	0	0	2.199	0.641	0.079
427	1	0	3.254	0.618	0.079
332	0	0	2.191	0.000	0.081
333	0	0	2.217	0.000	0.082
735	0	0	2.456	0.589	0.082
330	0	0	2.272	0.000	0.084
331	0	0	2.345	0.000	0.087
322	0	0	2.355	0.000	0.087
682	0	0	2.855	0.528	0.088
521	0	0	2.580	0.737	0.093
448	1	0	3.217	0.449	0.093
335	-1	0	1.991	-0.332	0.094
291	1	0	3.613	0.819	0.097
416	0	0	2.725	0.803	0.097
539	1	0	3.176	0.167	0.097
651	0	0	2.873	0.999	0.098
570	0	0	2.882	1.098	0.099
736	0	0	2.742	0.000	0.101
737	0	0	2.750	0.000	0.101
449	0	0	2.875	0.000	0.106
620	1	0	3.455	1.133	0.107
639	1	0	3.561	0.814	0.108

Table-A I-2 VSL indices for Hydro-Quebec network (Cont'd)

Bus number	Pi	Qi	Pmi	Qmi	VSL index
681	0	0	3.118	0.810	0.109
696	0	0	3.167	1.116	0.110
524	0	0	3.160	0.632	0.111
456	0	0	3.025	0.000	0.112
679	0	0	3.252	0.609	0.112
732	0	0	3.300	0.660	0.113
738	0	0	3.214	0.857	0.113
642	0	0	3.477	0.031	0.114
327	0	0	3.157	0.000	0.116
546	0	0	3.529	0.984	0.117
533	0	0	3.633	0.581	0.117
532	0	0	3.635	0.582	0.117
534	0	0	3.657	0.585	0.118
569	0	0	3.507	0.146	0.121
324	0	0	3.308	0.000	0.122
669	1	0	3.940	0.800	0.124
719	0	0	3.796	0.963	0.128
658	0	0	3.533	0.000	0.130
683	0	0	3.763	0.584	0.131
523	0	0	3.572	0.000	0.132
684	0	0	4.100	0.839	0.135
629	0	0	4.097	0.610	0.135
627	1	0	5.013	0.107	0.135
417	1	0	4.554	1.144	0.135
734	0	0	3.686	0.000	0.136
303	0	0	3.696	0.000	0.136
650	0	0	3.953	1.025	0.137
733	0	0	3.726	0.000	0.137

Table-A I-2 VSL indices for Hydro-Quebec network (Cont'd)

Bus number	Pi	Qi	Pmi	Qmi	VSL index
636	0	0	3.738	0.000	0.138
632	0	0	4.032	0.432	0.139
652	0	0	3.776	0.000	0.139
485	1	0	4.507	1.011	0.140
635	0	0	3.808	0.000	0.140
541	1	0	4.336	0.960	0.141
656	0	0	3.860	0.000	0.142
726	1	0	4.494	1.454	0.143
739	0	0	3.891	0.000	0.144
631	0	0	4.312	0.000	0.145
426	1	0	4.738	0.915	0.146
531	1	0	4.774	0.000	0.148
520	0	0	4.204	0.841	0.149
308	1	0	4.911	1.119	0.152
623	1	0	4.880	0.121	0.152
647	0	0	4.199	0.000	0.155
178	0	0	4.213	0.000	0.155
662	0	0	4.561	1.073	0.156
680	0	0	4.433	0.000	0.156
542	1	0	4.809	0.505	0.158
616	0	0	4.340	1.447	0.158
194	0	0	4.354	0.000	0.161
460	0	0	4.849	1.044	0.161
425	1	0	5.084	1.237	0.161
582	0	0	4.537	1.134	0.162
730	1	0	4.956	0.762	0.162
655	0	0	4.684	0.694	0.164
670	0	0	4.928	1.187	0.165

Table-A I-2 VSL indices for Hydro-Quebec network (Cont'd)

Bus number	Pi	Qi	Pmi	Qmi	VSL index
329	1	0	5.096	1.253	0.165
601	1	0	5.017	1.613	0.166
540	0	0	4.516	0.000	0.167
697	1	0	5.304	0.896	0.169
505	1	0	5.448	1.237	0.172
565	0	0	4.959	1.594	0.173
547	0	0	5.068	0.266	0.173
458	0	0	4.936	0.814	0.176
339	0	0	4.806	0.000	0.177
498	0	0	4.998	1.609	0.181
698	0	0	5.097	0.271	0.181
614	0	0	5.102	1.074	0.182
543	0	0	4.930	0.000	0.182
386	0	0	5.006	0.000	0.185
496	1	0	5.834	1.518	0.185
538	0	0	5.383	0.283	0.185
568	0	0	5.039	0.000	0.186
633	1	0	5.596	0.500	0.187
64	0	0	5.090	0.000	0.188
497	1	0	6.156	0.550	0.189
503	1	0	6.194	1.260	0.190
685	0	0	5.458	1.070	0.193
624	0	0	5.227	0.000	0.193
657	0	0	5.278	0.000	0.195
700	0	0	5.280	0.000	0.195
699	0	0	5.280	0.000	0.195
527	0	0	5.344	0.000	0.197
457	0	0	5.357	0.000	0.198

Table-A I-2 VSL indices for Hydro-Quebec network (Cont'd)

Bus number	Pi	Qi	Pmi	Qmi	VSL index
267	0	0	5.359	0.000	0.198
528	0	0	5.494	1.813	0.199
663	0	0	5.710	0.892	0.200
617	0	0	5.553	0.000	0.205
630	0	0	5.618	0.000	0.207
465	0	0	5.970	1.728	0.207
566	0	0	5.654	0.000	0.209
470	0	0	5.859	2.343	0.209
337	0	0	5.948	1.601	0.210
493	0	0	6.032	0.495	0.210
406	0	0	5.720	0.000	0.211
552	0	0	6.227	0.328	0.212
382	0	0	5.880	0.000	0.217
495	0	0	5.892	0.000	0.217
740	0	0	6.061	1.347	0.217
65	0	0	5.910	0.000	0.218
402	0	0	5.990	0.000	0.221
615	0	0	6.011	0.000	0.222
529	0	0	6.058	0.000	0.223
581	0	0	6.521	1.247	0.226
401	0	0	6.165	0.000	0.227
766	1	1	7.358	4.047	0.234
660	0	0	6.727	0.688	0.234
403	0	0	6.384	0.000	0.235
489	5	1	11.081	2.986	0.238
494	0	0	6.557	0.000	0.242
728	1	0	7.163	1.302	0.246
301	0	0	6.715	0.000	0.248

Table-A I-2 VSL indices for Hydro-Quebec network (Cont'd)

Bus number	Pi	Qi	Pmi	Qmi	VSL index
464	1	0	8.040	1.640	0.249
731	2	0	8.461	1.255	0.250
309	0	0	6.804	0.000	0.251
535	1	0	7.880	0.415	0.253
544	0	0	6.944	0.000	0.256
289	5	1	12.425	2.925	0.260
536	1	0	8.244	1.123	0.261
193	0	0	7.128	0.000	0.263
319	0	0	7.145	0.000	0.264
280	0	0	7.146	0.000	0.264
413	1	0	7.674	0.138	0.264
318	0	0	7.155	0.000	0.264
281	0	0	7.155	0.000	0.264
506	1	0	7.722	1.528	0.264
306	0	0	7.163	0.000	0.264
313	0	0	7.165	0.000	0.264
613	0	0	7.324	2.423	0.266
687	0	0	7.692	1.923	0.269
729	2	1	9.023	3.156	0.271
567	0	0	7.425	2.227	0.271
499	0	0	7.366	0.000	0.272
606	0	0	7.561	2.160	0.274
612	0	0	7.657	2.393	0.277
418	0	0	7.966	1.763	0.277
688	0	0	8.045	2.011	0.280
282	2	0	9.407	2.165	0.288
383	0	0	7.866	0.000	0.290
169	0	0	8.369	2.423	0.292

Table-A I-2 VSL indices for Hydro-Quebec network (Cont'd)

Bus number	Pi	Qi	Pmi	Qmi	VSL index
293	0	0	8.289	3.136	0.293
312	0	0	7.951	0.000	0.293
305	2	0	10.043	1.615	0.294
297	1	0	9.056	2.066	0.302
701	1	0	9.568	1.893	0.304
468	0	0	8.254	0.000	0.304
724	1	0	9.877	0.920	0.310
764	0	0	8.464	0.000	0.312
292	0	0	8.906	2.279	0.314
741	0	0	8.521	0.000	0.314
373	0	0	8.585	0.000	0.317
484	0	0	8.716	1.868	0.317
359	10	5	18.087	9.424	0.317
358	10	5	18.087	9.425	0.317
704	1	0	9.913	2.102	0.318
296	1	0	9.627	2.662	0.319
554	0	0	8.638	0.000	0.319
653	1	0	10.177	1.776	0.322
727	0	0	8.734	0.000	0.322
583	1	0	9.769	2.322	0.324
488	3	1	11.376	5.333	0.325
611	0	0	8.841	0.000	0.326
423	1	0	9.805	3.051	0.327
659	0	0	8.877	0.000	0.327
580	1	0	9.835	0.573	0.328
307	0	0	8.976	0.000	0.331
537	0	0	9.121	0.000	0.336
147	5	0	13.924	0.000	0.338

Table-A I-2 VSL indices for Hydro-Quebec network (Cont'd)

Bus number	Pi	Qi	Pmi	Qmi	VSL index
148	5	0	13.924	0.000	0.338
618	1	0	10.485	3.175	0.338
278	3	0	12.260	1.802	0.339
272	10	2	19.630	3.899	0.340
722	0	0	9.214	0.000	0.340
723	0	0	9.214	0.000	0.340
260	6	1	15.748	3.432	0.341
421	1	0	10.358	2.379	0.342
725	0	0	9.275	0.000	0.342
469	0	0	9.821	2.405	0.348
279	0	0	9.427	0.000	0.348
419	0	0	9.847	2.928	0.348
571	1	0	10.946	1.473	0.351
609	0	0	9.631	0.000	0.355
411	0	0	9.668	0.000	0.357
689	0	0	9.725	0.000	0.359
163	0	0	9.725	0.000	0.359
284	2	0	11.808	2.662	0.359
283	2	0	11.688	0.063	0.361
578	0	0	9.796	0.000	0.361
587	1	0	10.570	2.292	0.362
579	0	0	9.814	0.000	0.362
420	0	0	9.833	0.000	0.363
351	0	0	9.871	0.000	0.364
626	0	0	10.079	0.000	0.372
288	1	0	11.608	0.185	0.373
341	0	0	10.146	0.000	0.374
466	0	0	10.147	0.000	0.374

Table-A I-2 VSL indices for Hydro-Quebec network (Cont'd)

Bus number	Pi	Qi	Pmi	Qmi	VSL index
166	0	0	10.158	0.000	0.375
584	0	0	10.657	0.000	0.376
573	1	0	10.785	0.506	0.376
605	0	0	10.208	0.000	0.377
574	0	0	10.245	0.000	0.378
415	2	0	12.154	2.000	0.378
575	0	0	10.279	0.000	0.379
285	6	1	16.690	1.425	0.380
619	0	0	10.320	0.000	0.381
264	6	1	16.235	2.762	0.383
294	0	0	10.431	0.000	0.385
259	6	1	16.550	4.057	0.385
265	6	1	16.723	1.983	0.386
325	0	0	10.509	0.000	0.388
295	1	0	11.206	1.499	0.388
326	0	0	10.547	0.000	0.389
164	0	0	10.557	0.000	0.389
323	0	0	10.665	0.000	0.393
621	0	0	11.169	0.536	0.394
314	0	0	10.736	0.000	0.396
277	4	1	14.507	2.224	0.397
165	0	0	10.858	0.000	0.401
551	0	0	11.341	0.597	0.405
703	0	0	11.255	2.811	0.406
271	6	1	17.192	3.984	0.410
560	0	0	11.137	0.000	0.411
562	0	0	11.142	0.000	0.411
561	0	0	11.142	0.000	0.411

Table-A I-2 VSL indices for Hydro-Quebec network (Cont'd)

Bus number	Pi	Qi	Pmi	Qmi	VSL index
622	0	0	11.186	0.000	0.413
298	2	0	13.514	1.769	0.413
304	0	0	11.230	0.000	0.414
486	1	0	11.833	4.142	0.416
376	0	0	11.429	2.271	0.416
661	0	0	11.350	0.000	0.419
585	0	0	11.357	0.000	0.419
586	0	0	11.385	0.000	0.420
492	0	0	11.455	3.818	0.421
548	0	0	11.566	0.000	0.427
371	1	0	12.243	0.428	0.428
317	0	0	11.638	0.000	0.429
276	7	1	18.274	3.892	0.430
550	0	0	11.692	0.000	0.431
316	1	0	13.196	4.179	0.433
258	0	0	11.748	0.000	0.433
500	1	0	12.315	3.131	0.434
467	0	0	11.811	0.000	0.436
549	0	0	11.879	0.000	0.438
400	0	0	11.955	0.000	0.441
463	0	0	12.446	2.855	0.444
342	0	0	12.058	0.000	0.445
666	1	0	13.491	3.059	0.448
344	2	1	13.768	5.455	0.449
346	2	1	14.254	4.417	0.451
502	3	1	15.688	2.366	0.451
345	4	1	16.194	4.989	0.453
607	1	0	13.449	2.690	0.455

Table-A I-2 VSL indices for Hydro-Quebec network (Cont'd)

Bus number	Pi	Qi	Pmi	Qmi	VSL index
664	1	0	13.283	3.170	0.460
608	1	0	13.070	2.655	0.460
422	0	0	12.481	0.000	0.460
275	8	2	20.728	3.995	0.461
168	0	0	12.521	0.000	0.462
263	2	0	14.699	2.050	0.468
343	0	0	12.881	0.000	0.475
702	0	0	12.913	0.000	0.476
404	0	0	12.914	0.000	0.476
286	3	0	15.481	0.974	0.478
211	0	0	12.978	0.000	0.479
385	0	0	13.094	0.000	0.483
405	0	0	13.112	0.000	0.484
137	3	0	15.671	0.000	0.486
384	0	0	13.199	0.000	0.487
604	0	0	13.320	0.000	0.491
391	0	0	13.394	0.000	0.494
409	0	0	13.402	0.000	0.494
175	0	0	13.478	0.000	0.497
315	0	0	13.512	0.000	0.498
290	4	1	17.562	4.445	0.499
597	1	0	14.315	1.859	0.502
690	0	0	13.853	1.301	0.504
209	0	0	13.933	0.000	0.514
692	0	0	13.983	0.000	0.516
287	0	0	14.001	0.000	0.516
598	0	0	14.353	1.511	0.516
210	0	0	14.007	0.000	0.517

Table-A I-2 VSL indices for Hydro-Quebec network (Cont'd)

Bus number	Pi	Qi	Pmi	Qmi	VSL index
491	0	0	14.146	0.000	0.522
490	0	0	14.146	0.000	0.522
501	0	0	14.334	2.118	0.522
691	0	0	14.156	0.000	0.522
310	0	0	14.174	0.000	0.523
186	0	0	14.239	0.000	0.525
187	0	0	14.239	0.000	0.525
269	2	0	16.451	0.925	0.527
207	0	0	14.287	0.000	0.527
216	0	0	14.288	0.000	0.527
206	0	0	14.352	0.000	0.529
215	0	0	14.353	0.000	0.529
410	1	0	15.185	5.121	0.531
311	0	0	14.428	0.000	0.532
603	0	0	14.457	0.000	0.533
185	0	0	14.495	0.000	0.535
184	0	0	14.495	0.000	0.535
471	1	0	15.172	3.707	0.537
472	1	0	15.827	0.713	0.543
274	8	2	23.187	4.898	0.543
665	0	0	15.250	0.400	0.546
273	7	1	21.671	1.767	0.546
676	0	0	15.069	3.129	0.546
300	2	0	16.417	2.920	0.549
195	0	0	14.923	0.000	0.550
387	0	0	14.970	0.000	0.552
270	0	0	14.984	0.000	0.553
174	0	0	15.003	0.000	0.553

Table-A I-2 VSL indices for Hydro-Quebec network (Cont'd)

Bus number	Pi	Qi	Pmi	Qmi	VSL index
266	1	0	16.083	3.243	0.555
320	0	0	15.113	0.000	0.557
321	0	0	15.124	0.000	0.558
599	0	0	15.237	0.000	0.562
600	0	0	15.242	0.000	0.562
591	2	0	17.159	4.393	0.562
257	0	0	15.280	0.000	0.564
712	2	0	17.253	3.758	0.568
368	0	0	15.418	0.000	0.569
693	0	0	15.379	-17.668	0.569
299	2	0	17.296	1.847	0.569
379	3	0	17.999	3.367	0.569
366	0	0	15.439	0.000	0.569
388	2	0	17.527	1.959	0.569
474	2	0	17.600	3.443	0.571
140	0	0	15.589	0.000	0.575
161	0	0	15.598	0.000	0.575
367	0	0	15.669	0.000	0.578
588	2	0	17.586	4.503	0.578
154	2	0	18.143	3.601	0.578
711	1	0	16.604	3.487	0.578
713	2	0	17.669	2.477	0.579
395	1	0	16.221	2.986	0.579
476	1	0	16.221	2.986	0.579
714	1	0	16.692	2.385	0.580
480	0	0	15.932	3.414	0.583
479	0	0	15.932	3.414	0.583
716	2	0	17.819	2.101	0.585

Table-A I-2 VSL indices for Hydro-Quebec network (Cont'd)

Bus number	Pi	Qi	Pmi	Qmi	VSL index
374	0	0	15.895	0.000	0.586
715	2	0	17.896	3.292	0.588
389	4	1	20.133	6.325	0.589
350	0	0	16.008	0.000	0.590
595	0	0	16.410	0.995	0.594
596	0	0	16.410	0.995	0.594
473	1	0	17.403	3.385	0.595
397	0	0	16.149	0.000	0.596
381	0	0	16.182	0.000	0.597
364	6	2	22.197	5.967	0.597
365	1	0	17.502	4.376	0.599
710	0	0	16.266	0.000	0.600
152	2	1	18.738	4.755	0.600
709	0	0	16.277	0.000	0.600
392	0	0	16.284	0.000	0.601
179	0	0	16.285	0.000	0.601
180	0	0	16.285	0.000	0.601
352	0	0	16.297	0.000	0.601
302	0	0	16.311	0.000	0.602
706	2	1	18.288	5.213	0.602
171	3	0	19.446	1.689	0.602
481	0	0	16.332	0.000	0.602
482	0	0	16.332	0.000	0.602
182	0	0	16.388	4.975	0.603
589	0	0	16.366	0.000	0.604
393	1	0	17.592	1.329	0.604
153	0	0	16.421	0.000	0.606
189	0	0	16.427	0.000	0.606

Table-A I-2 VSL indices for Hydro-Quebec network (Cont'd)

Bus number	Pi	Qi	Pmi	Qmi	VSL index
188	0	0	16.427	0.000	0.606
370	0	0	16.827	4.407	0.606
158	0	0	16.461	0.000	0.607
363	0	0	16.468	0.000	0.607
590	0	0	16.471	0.000	0.608
173	0	0	16.484	0.000	0.608
478	0	0	16.504	0.000	0.609
477	0	0	16.504	0.000	0.609
593	0	0	16.514	0.000	0.609
594	0	0	16.514	0.000	0.609
717	0	0	16.539	0.000	0.610
718	0	0	16.539	0.000	0.610
170	0	0	16.559	0.000	0.611
149	0	0	16.574	0.000	0.611
176	0	0	16.586	0.000	0.612
177	0	0	16.588	0.000	0.612
705	2	0	18.562	4.164	0.612
667	0	0	16.846	5.615	0.613
602	0	0	16.678	0.000	0.615
377	0	0	16.722	0.000	0.617
390	0	0	16.772	0.000	0.619
190	0	0	16.796	0.000	0.620
191	0	0	16.796	0.000	0.620
151	0	0	16.868	0.000	0.622
380	0	0	16.868	0.000	0.622
353	0	0	16.877	0.000	0.623
142	0	0	16.918	0.000	0.624
150	0	0	16.930	0.000	0.624

Table-A I-2 VSL indices for Hydro-Quebec network (Cont'd)

Bus number	Pi	Qi	Pmi	Qmi	VSL index
127	0	0	16.950	0.000	0.625
512	0	0	17.389	4.549	0.625
360	0	0	16.973	0.000	0.626
181	0	0	16.993	0.000	0.627
592	3	0	19.851	0.642	0.627
396	2	0	19.112	4.062	0.628
720	0	0	17.062	0.000	0.629
721	0	0	17.062	0.000	0.629
134	0	0	17.063	0.000	0.629
514	3	1	20.203	6.653	0.629
610	0	0	17.065	0.000	0.629
121	0	0	17.078	0.000	0.630
708	0	0	17.092	0.000	0.630
707	0	0	17.094	0.000	0.630
203	0	0	17.117	0.000	0.631
204	0	0	17.125	0.000	0.632
167	0	0	17.141	0.000	0.632
132	0	0	17.147	0.000	0.632
513	4	1	20.773	6.755	0.633
399	0	0	17.168	0.000	0.633
475	0	0	17.180	0.000	0.634
361	0	0	17.230	0.000	0.636
218	0	-2	17.271	0.000	0.637
183	0	0	17.282	0.000	0.637
120	0	0	17.294	0.000	0.638
394	0	0	17.300	0.000	0.638
378	0	0	17.300	0.000	0.638
357	0	0	17.403	0.000	0.642

Table-A I-2 VSL indices for Hydro-Quebec network (Cont'd)

Bus number	Pi	Qi	Pmi	Qmi	VSL index
362	0	0	17.422	0.000	0.643
247	0	0	17.427	0.000	0.643
205	0	0	17.558	0.000	0.648
214	0	0	17.567	0.000	0.648
509	2	0	19.424	3.664	0.651
369	0	0	17.693	0.000	0.653
518	1	0	19.065	3.709	0.654
225	0	1	17.731	0.000	0.654
398	1	0	18.675	3.882	0.654
519	1	0	19.180	0.971	0.654
372	0	0	17.753	0.000	0.655
510	1	0	18.640	3.532	0.655
355	0	0	17.774	0.000	0.656
133	0	0	17.793	0.000	0.656
356	1	0	19.222	3.938	0.659
354	3	0	20.754	2.824	0.659
243	0	-1	17.862	0.000	0.659
233	0	4	17.866	0.000	0.659
516	1	0	19.302	3.755	0.662
241	0	3	17.966	0.000	0.663
208	0	0	17.988	0.000	0.663
515	1	0	19.299	3.750	0.664
238	0	3	18.009	0.000	0.664
224	0	2	18.055	0.000	0.666
219	0	5	18.082	0.000	0.667
517	1	0	19.378	3.765	0.667
157	0	0	18.111	0.000	0.668
230	0	6	18.143	0.000	0.669

Table-A I-2 VSL indices for Hydro-Quebec network (Cont'd)

Bus number	Pi	Qi	Pmi	Qmi	VSL index
248	0	0	18.167	0.000	0.670
347	1	0	19.059	4.327	0.671
139	0	0	18.182	0.000	0.671
511	4	1	21.798	3.491	0.671
507	0	0	18.203	0.000	0.671
159	0	0	18.203	0.000	0.671
508	0	0	18.206	0.000	0.672
122	0	0	18.226	0.000	0.672
123	0	0	18.269	0.000	0.674
340	5	0	23.355	2.424	0.687
160	0	0	18.699	0.000	0.690
745	0	0	18.729	0.000	0.691
221	0	1	18.750	0.000	0.692
231	0	2	18.776	0.000	0.693
755	0	0	18.822	0.000	0.694
771	0	0	18.822	0.000	0.694
758	0	0	18.830	0.000	0.695
220	0	8	18.887	0.000	0.697
229	0	6	18.946	0.000	0.699
130	0	0	19.005	0.000	0.701
781	0	0	19.076	0.000	0.704
232	0	2	19.138	0.000	0.706
756	0	0	19.182	0.000	0.708
746	0	0	19.197	0.000	0.708
757	0	0	19.248	0.000	0.710
239	0	10	19.256	0.000	0.710
772	0	0	19.313	0.000	0.712
131	0	0	19.330	0.000	0.713

Table-A I-2 VSL indices for Hydro-Quebec network (Cont'd)

Bus number	Pi	Qi	Pmi	Qmi	VSL index
747	0	0	19.335	0.000	0.713
783	0	0	19.341	0.000	0.713
744	0	0	19.362	0.000	0.714
754	0	0	19.362	0.000	0.714
773	0	0	19.401	0.000	0.716
759	0	0	19.404	0.000	0.716
770	0	0	19.450	0.000	0.717
780	0	0	19.486	0.000	0.719
228	0	5	19.537	0.000	0.721
778	0	0	19.630	0.000	0.724
156	0	0	19.660	0.000	0.725
751	0	0	19.675	0.000	0.726
246	0	11	19.685	0.000	0.726
138	0	0	19.688	0.000	0.726
749	0	0	19.748	0.000	0.728
761	0	0	19.748	0.000	0.728
774	0	0	19.754	0.000	0.729
338	0	0	20.163	5.367	0.729
763	0	0	19.794	0.000	0.730
776	0	0	19.795	0.000	0.730
196	0	0	19.831	0.000	0.731
245	0	7	19.881	0.000	0.733
200	0	0	19.884	0.000	0.733
201	0	0	19.894	0.000	0.734
348	0	0	19.904	0.000	0.734
244	0	4	19.927	0.000	0.735
212	0	0	19.971	0.000	0.737
762	0	0	19.985	0.000	0.737

Table-A I-2 VSL indices for Hydro-Quebec network (Cont'd)

Bus number	Pi	Qi	Pmi	Qmi	VSL index
775	0	0	19.985	0.000	0.737
223	0	-7	20.007	0.000	0.738
192	0	0	20.094	0.000	0.741
146	0	0	20.105	0.000	0.742
155	0	0	20.205	0.000	0.745
199	0	0	20.247	0.000	0.747
124	0	0	20.264	0.000	0.747
234	0	0	20.280	0.000	0.748
222	0	3	20.323	0.000	0.750
125	0	0	20.367	0.000	0.751
750	0	0	20.410	0.000	0.753
135	0	0	20.414	0.000	0.753
742	0	0	20.428	0.000	0.753
235	0	-1	20.475	0.000	0.755
237	0	-3	20.496	0.000	0.756
145	0	0	20.499	0.000	0.756
143	0	0	20.524	0.000	0.757
779	0	0	20.554	0.000	0.758
752	0	0	20.585	0.000	0.759
768	0	0	20.585	0.000	0.759
172	0	0	20.591	0.000	0.760
236	0	4	20.624	0.000	0.761
240	0	2	20.635	0.000	0.761
136	0	0	20.673	0.000	0.763
777	0	0	20.688	0.000	0.763
197	0	0	20.738	0.000	0.765
782	0	0	20.824	0.000	0.768
129	0	0	20.856	0.000	0.769

Table-A I-2 VSL indices for Hydro-Quebec network (Cont'd)

Bus number	Pi	Qi	Pmi	Qmi	VSL index
226	0	17	20.915	0.000	0.771
769	0	0	20.981	0.000	0.774
753	0	0	20.982	0.000	0.774
743	0	0	20.983	0.000	0.774
227	0	11	21.267	0.000	0.784
126	0	0	21.312	0.000	0.786
128	0	0	21.322	0.000	0.786
242	0	0	21.413	0.000	0.790
61	0	0	21.590	4.048	0.790
407	0	0	21.609	0.000	0.797
198	0	0	21.696	0.000	0.800
144	0	0	22.315	0.000	0.823
408	3	0	25.605	3.336	0.840
261	0	0	25.316	0.000	0.934
141	0	0	27.111	0.000	1.000

LIST OF REFERENCES

- Abed, A. M. (1999). WSCC voltage stability criteria, undervoltage load shedding strategy, and reactive power reserve monitoring methodology. Power Engineering Society Summer Meeting, 1999. IEEE, IEEE.
- Canizares, C. A. (2002). "Voltage stability assessment: concepts, practices and tools." Power System Stability Subcommittee Special Publication IEEE/PES, Final Document (thunderbox.uwaterloo.ca/~claudio/claudio.html# VSWG).
- Chakrabarti, A. (2010). An introduction to reactive power control and voltage stability in power transmission systems, PHI Learning Pvt. Ltd.
- Committee, I. P. S. E. (1990). Voltage stability of power systems: concepts, analytical tools, and industry experience, IEEE.
- Cutsem, T. V. and C. Vournas (1998). Voltage stability of electric power systems. Boston, Kluwer Academic Publishers.
- Fairley, P. (2004). "The unruly power grid." Spectrum, IEEE **41**(8): 22-27.
- Gao, B., G. Morison and P. Kundur (1992). "Voltage stability evaluation using modal analysis." Power Systems, IEEE Transactions on **7**(4): 1529-1542.
- Gao, B., G. Morison and P. Kundur (1996). "Towards the development of a systematic approach for voltage stability assessment of large-scale power systems." IEEE transactions on power systems **11**(3): 1314-1324.
- Hussein, K., I. Muta, T. Hoshino and M. Osakada (1995). "Maximum photovoltaic power tracking: an algorithm for rapidly changing atmospheric conditions." IEE Proceedings-Generation, Transmission and Distribution **142**(1): 59-64.
- Kessel, P. and H. Glavitsch (1986). "Estimating the voltage stability of a power system." Power Delivery, IEEE Transactions on **1**(3): 346-354.
- Kundur, P. (1999). "Voltage stability assessment, procedures and guides,". IEEE/PES Power System Stability Subcommittee Special Publication.
- Kundur, P., N. J. Balu and M. G. Lauby (1994). Power system stability and control. New York ; Montréal, McGraw-Hill.
- Kundur, P., J. Paserba, V. Ajjarapu, G. Andersson, A. Bose, C. Canizares, N. Hatziargyriou, D. Hill, A. Stankovic and C. Taylor (2004). "Definition and classification of power system stability IEEE/CIGRE joint task force on stability terms and definitions." Power Systems, IEEE Transactions on **19**(3): 1387-1401.
- Kwatny, H. G., A. Pasrija and L. Bahar (1986). "Static bifurcations in electric power networks: loss of steady-state stability and voltage collapse." Circuits and Systems, IEEE Transactions on **33**(10): 981-991.
- Lagace, P. (2012). Power flow methods for improving convergence. IECON 2012-38th Annual Conference on IEEE Industrial Electronics Society, IEEE.
- Lof, P.-A., G. Andersson and D. Hill (1993). "Voltage stability indices for stressed power systems." Power Systems, IEEE Transactions on **8**(1): 326-335.
- Lof, P.-A., T. Smed, G. Andersson and D. Hill (1992). "Fast calculation of a voltage stability index." Power Systems, IEEE Transactions on **7**(1): 54-64.

- Mahseredjian, J. (2012). Power transfer between two points and analysis of voltage stability. [Notes du cours Comportement des réseaux électriques]. Montreal, École Polytechnique de Montréal.
- Rodrigues, A. B., R. B. Prada and M. Da Guia da Silva (2010). "Voltage stability probabilistic assessment in composite systems: Modeling unsolvability and controllability loss." Power Systems, IEEE Transactions on **25**(3): 1575-1588.
- Tamura, Y., H. Mori and S. Iwamoto (1983). "Relationship between voltage instability and multiple load flow solutions in electric power systems." Power Apparatus and Systems, IEEE Transactions on(5): 1115-1125.
- Taylor, C. W. (1994). Power system voltage stability, McGraw-Hill.
- Thomas, R. J. and A. Tiranuchit (1986). Voltage instabilities in electric power networks. Proc. Eighteenth Southeast Symposium on System Theory.
- Tiwari, A. and V. Ajjarapu (2007). Contingency assessment for voltage dip and short term voltage stability analysis. Bulk Power System Dynamics and Control-VII. Revitalizing Operational Reliability, 2007 iREP Symposium, IEEE.
- Venikov, V., V. Stroeve, V. Idelchick and V. Tarasov (1975). "Estimation of electrical power system steady-state stability in load flow calculations." Power Apparatus and Systems, IEEE Transactions on **94**(3): 1034-1041.
- Vu, K., M. M. Begovic, D. Novosel and M. M. Saha (1999). "Use of local measurements to estimate voltage-stability margin." Power Systems, IEEE Transactions on **14**(3): 1029-1035.